Australian Government
Department of Defence
Defence Science and
Technology Organisation

Maritime Laser Communications Trial 98152-19703

Kenneth J. Grant, Kerry A. Mudge, Bradley A. Clare, Anna S. Perejma and Wayne M. Martinsen

Command, Control, Communications and Intelligence Division
Defence Science and Technology Organisation

DSTO-GD-0686

ABSTRACT

This General Document describes the objectives, methodology, and results of Maritime Laser Communications Trial 98152-19703 held at Port Wakefield Proof & Experimental Establishment in September 2011. A novel analogue FM ship-to-shore communications system was used to demonstrate video and bidirectional audio transmission up to 3km.

RELEASE LIMITATION

Approved for Public Release

Published by

Command, Control, Communications and Intelligence Division
DSTO Defence Science and Technology Organisation
PO Box 1500
Edinburgh South Australia 5111 Australia

Telephone: (08) 7389 5555
Fax: (08) 7389 6567

AR 015-320
June 2012

APPROVED FOR PUBLIC RELEASE

Maritime Laser Communications Trial 98152-19703

Executive Summary

There is increasing interest in free space optical communications (FSOC) as an alternative to fibre optics and radio frequency communications, particularly for 'last mile' applications and applications with size, weight and power restrictions. The potential advantages of free space optical communications include high bandwidth, no spectrum licensing issues, smaller lighter payloads, low probability of intercept and immunity from interference / jamming.

As part of Task 07/009 *Communications Support to Capability Development*, C3I Division is researching concepts and technologies that can be applied to laser communications in the maritime environment. Compared to operating over land, the maritime environment offers significant advantages in that it usually provides line-of-sight conditions, which is required for FSOC, and its atmospheric scintillation noise is typically one to two orders of magnitude lower.

This General Document describes the objectives, methodology, and results of *Maritime Laser Communications Trial 98152-19703* held at Port Wakefield Proof & Experimental Establishment in September 2011. The primary objective of the trial was to demonstrate ship-to-shore optical communications, as an intermediate step to ship-to-ship communications. This work is underpinned by the modulating retroreflector (MRR), which allows high bandwidth optical communication using a laser system at only one end of the link. DSTO has a close collaboration with the US Naval Research Laboratories (NRL) in FSOC, and the optical link demonstrated in the trial used an MRR on loan from NRL, under the auspices of a TTCP (The Technical Cooperation Program) equipment and material transfer.

During this trial an eye-safe, free space optical ship-to-shore communications link was successfully demonstrated. In particular, a novel FM audio/video communication system successfully operated at a transmission distance of 3 km. This is, to our knowledge, the first demonstration of a bidirectional audio/video link using modulating retro-reflectors.

These measurements indicate that this FSOC system is a feasible technology for the Royal Australian Navy. It has the potential to provide additional capabilities, such as: communication during EMCON conditions; provision of a redundant communications channel; and bandwidth intensive network centric operations. Further, the technology demonstrated in this trial can be readily extended to ship-to-ship communications.

This page is intentionally blank

Contents

1. Introduction

There is increasing interest in free space optical communications (FSOC) as an alternative to fibre optics and radio frequency communications, particularly for 'last mile' applications and applications with size, weight and power restrictions. The potential advantages of free space optical communications include high bandwidth, no spectrum licensing issues, smaller lighter payloads, low probability of intercept and immunity from interference / jamming.

As part of Task 07/009 *Communications Support to Capability Development*, C3I Division is researching concepts and technologies that can be applied to laser communications in the maritime environment. Compared to operating over land, the maritime environment offers significant advantages in that it usually provides line-of-sight conditions, which is required for FSOC, and its atmospheric scintillation noise is typically one to two orders of magnitude lower.

This work is underpinned by the modulating retro-reflector (MRR) which was developed by the US Naval Research Laboratories (NRL). MRRs are capable of supporting both analogue and digital communications and are protocol-independent.

DSTO has a close collaboration with NRL which has given the Department of Defence access to key technologies in this field. Dr Grant was on long term attachment to NRL from 2004 to 2006, and we have subsequently conducted joint DSTO-NRL FSOC trials under the auspices of TTCP. NRL has lent DSTO an MRR as a TTCP equipment & material transfer (E&MT), and in 2009 we purchased the first NovaSol optical interrogator to be released outside the USA.

2. Background

Free space optical communication offers several potential benefits for Naval platforms. In particular, high data rate communication (up to several Gbps) could be established between surface vessels, as well as between a surface vessel and unmanned aerial vehicles (UAVs), airborne platforms, land forces and potentially satellites. The ability to connect two or more platforms in a high speed network provides enhanced operational flexibility and is an enabling technology for network centric warfare applications.

Free space optical communications is a natural candidate for maritime applications due to the availability of line-of-sight to the horizon. This potentially could be extended to longer ranges by communicating via a UAV or other airborne platform. The low divergence of the optical transmitters (typically 0.1 to 5 milliradians) implies a low probability of detection and interception (LPD and LPI). In addition, FSOC systems have a high resistance to jamming, since the receivers have narrow fields-of-view. With attention to EM shielding, they are immune to conventional RF jamming techniques, have no spectrum licensing restrictions and in general have power, weight and size requirements that are

low relative to the equivalent RF systems. This presents an opportunity for FSOC technologies to serve as an adjunct capability to RF communications, for line-of-sight (LOS) applications or under conditions of radio silence or emission control (EMCON).

Current FSOC systems typically operate at a near infrared wavelength of 1.5 μm, invisible to the eye. This wavelength is chosen, in part, in order to leverage transmitter technology from long-haul fibre optic communications, which also operates at this wavelength, but importantly this wavelength also has low atmospheric absorption. It is undetectable by conventional night vision equipment and infrared surveillance cameras as it requires specialised InGaAs cameras and sensors for detection.

There are several challenges for development of practical FSOC systems for naval applications. Due to the low divergence of the optical transmitters, precise pointing and tracking is required. There is also the potential for signal attenuation due to scattering and absorption caused by fog, rain and sea spray. Signal attenuation may be addressed by system design for the required propagation distance and environment. Parameters to consider are the transmitter power and divergence, receiver aperture size, sensitivity and signal processing. These can all be adjusted to ensure a sufficient link margin for a viable FSOC solution.

In clear weather conditions, the effects of atmospheric turbulence become the dominant challenge. Atmospheric turbulence is caused by localised temperature fluctuations in the air, leading to small changes in refractive index. The index variation creates a series of weak lenses in the optical path resulting in time varying scintillation effects in the optical beam. This causes fluctuations in the received signal strength (up to 30dB in magnitude) and increased laser beam divergence [1]. The strength of the atmospheric turbulence varies significantly with prevailing weather conditions and time of day and is characterised by the refractive index structure parameter C_n^2. Atmospheric turbulence effects are typically much lower over water than over land and can be mitigated by use of large receiver apertures, adaptive optics, multiple transmitters or receivers, and forward error correction coding.

Commercial FSOC point-to-point Ethernet links, up to 1 Gbps, have been available for some time. Manufacturers include fSONA, Canon, Lightpointe, Terabeam, AirFiber and AOptix. These commercial systems are primarily engineered to be placed on fixed structures such as buildings. Hence, their pointing and tracking is only required to overcome misalignments due to building sway caused by wind and temperature changes. For military applications more sophisticated pointing, acquisition and tracking systems are required to enable use on mobile platforms such as ships, vehicles or airplanes to compensate for movement caused by platform mobility, platform vibration, rough sea states or uneven terrain [2]. Currently three companies are developing tracking systems ruggedised for military use, viz. NovaSol (www.nova-sol.com), Carl Zeiss Optronics GmbH (www.zeiss.de) and AOptix (www.aoptix.com). The NovaSol system was used in the current trial.

FSOC systems in the maritime environment have been demonstrated to operate reliably in several reports. In [3] laser communication was successfully demonstrated during Trident Warrior 06 between ships *USS Bonhomme Richard* and *USS Denver*. Video was transmitted

between the laser communication terminals at data rates of 300 Mbps. Error free video was received at ranges of 9.3 km and at the maximum tested range of 17.6 km, minor defects in the video were observed. In [4], laser communication was demonstrated from ship to shore at ranges from 2 to 22 km. Using an AOptix LCT-5 terminal data rates of 10 Gbps were transmitted, with a predicted throughput of 90%. In [5], several sea trials of Zeiss Optronics terminals were reported, with a data rate of 70 Mbps at 18 km successfully demonstrated.

There are two distinct modes of operation of FSOC systems, namely the 'point-to-point' or 'symmetric' mode and the 'retro-reflector' mode also termed the 'asymmetric' mode. In the point-to-point links two symmetrical optical transceivers are used at either end of the link. This mode has the advantage of long range and high data-rate due to high antenna gain, but requires very accurate pointing, acquisition and tracking. For small platforms such as UAVs and unattended sensors with low size, weight and power (SWAP) requirements, it may not be possible to have a large transceiver terminal at both ends of the link. In this case, the two ends of the link are asymmetric in size, with one end capable of having a large FSOC terminal, due to the available resources of a ship or ground station, whereas the other end, a UAV for example, requires a light weight, low power system. In these cases an asymmetric or retro-reflector link is advantageous. The retro-reflector system consists of an intensity modulator (or absorption modulator) combined with an optical retro-reflector, forming a modulating retro-reflector (MRR). This enables an optical interrogating beam from a remote optical transceiver to be encoded with information via intensity modulation that is then reflected back to the source. The asymmetric system has the advantage of greatly reduced pointing and tracking requirements, since the retroreflector obviates the need for pointing and tracking at the MRR end of the link. Furthermore, the retro-reflector end of the link is a low power, passive device in that it does not radiate, and only transmits information when illuminated with a beam of the correct wavelength. An asymmetric link using an MRR has some disadvantages compared to a point-to-point link. Firstly, the bandwidth of the link is limited by the speed of the absorption modulator to typically 10 Mbps. Second, the range of the link is reduced, as the received signal is inversely proportional to the 4^{th} power of the range (similar to a radar signal).

The MRR can encode information using either analogue or digital formats. One of the benefits of using an analogue system is the reduced bandwidth and power requirements, compared to a digital equivalent. Furthermore the "graceful degradation" of analogue systems is a well-known advantage for many applications. DSTO has been developing analogue audio and video modulation for FSOC links for several years. Initial attempts at using amplitude modulated signals were susceptible to degradation caused by amplitude variations due to atmospheric turbulence [6]. To mitigate these effects, a custom designed frequency modulated analogue video/audio system was developed at DSTO primarily for use with MRR devices [7]. This system was demonstrated to operate successfully using a passive retro-reflector in the terrestrial environment over a 1.5 km range. In a joint demonstration with NRL at their Chesapeake Bay facility, it was also demonstrated in the maritime environment over a range of 16 km [8]. Recently, this FM Audio/Video system was demonstrated to operate successfully using a 6.3 mm diameter MRR at the DSTO laser range facility at Edinburgh SA over a range of 1.5 km. In this demonstration the transmitted video was free from scintillation induced artefacts for C_n^2 up to 2×10^{-14} $m^{-2/3}$,

and was useable (with some artefacts and drop-outs) for C_n^2 up to 2 x 10^{-13} $m^{-2/3}$ [7][12]. Demonstration of this system in a ship-to-shore configuration was one of the objectives of the current trial.

3. Trial Objectives

The primary objective of the trial was to demonstrate ship-to-shore optical communications, as an intermediate step to ship-to-ship communications. The aims of the trial therefore were to:

- Demonstrate land-to-land FSOC across water
- Test the ability of the NovaSol dual-mode optical interrogator (DMOI transceiver) on a boat to track a retro-reflector on shore
- Test the ability of NovaSol optical interrogator on shore to track a retro-reflector on a boat
- Test novel FM audio/video communication system at different ranges
- Test the ability to maintain a ship-to-shore lasercomm link at different ranges
- Achieve a video and audio link at a range of two nautical miles, or 3.7 km

The performance of the ship-to-shore optical communication system was assessed by analysing the captured audio and video.

4. Trial Methodology

The optical communication system demonstrated was a 10 MHz FM audio/video link using an MRR. In addition a two-way audio link was demonstrated between the MRR and the optical interrogator by imparting a low amplitude, 60 kHz FM modulation on the interrogating laser beam that was detected by a separate photodetector and audio demodulator co-located with the MRR. A schematic diagram of the experimental setup is shown in Figure 1. The diagram illustrates the connections between the interrogator (DMOI), MRR and relevant electronics. In Figure 1 the beam transmitted from the interrogator is coloured yellow to represent the 60 kHz audio modulation applied to the laser using a fibre-coupled modulator (Brimrose AMM-100-8-70-1550-3FP). This beam is received by the detector, labelled optical Rx. The beam coloured red, is the part of the transmit (yellow) beam that is retro-reflected from the MRR, and encoded with a 10 MHz FM modulation signal. The red beam is collected by the optical receiver in the interrogator and directed by optical fibre to the pinfet detector. The main components are discussed in detail in Section 4.2.

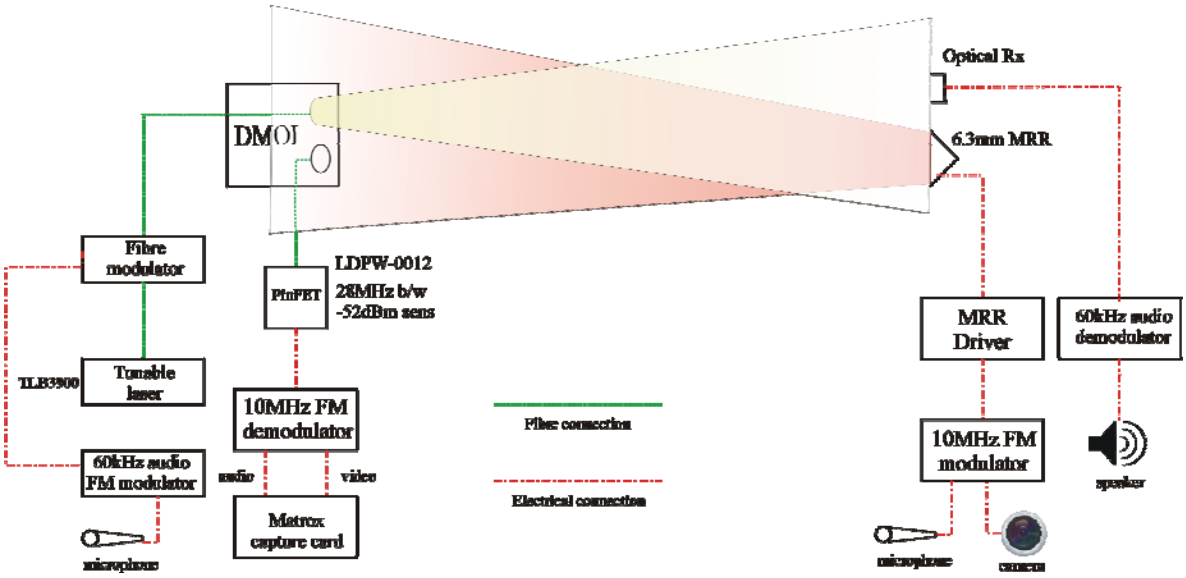

Figure 1 Schematic of the experimental setup used in the trial

The trial took place during the daylight hours of 19 to 23 September, 2011 at the Port Wakefield Proof and Experimental Establishment (PWP&EE), South Australia. PWP&EE is located approximately 100 km north of Adelaide, and conducts weapons research and testing for the Australian Army and Navy. The main advantage to this work was the fact the range includes an area approximately 18 km x 5 km adjacent to the shore which is prohibited to civilian vessels (Figure 2, Figure 3). This mitigates the risk of inadvertent exposure to laser radiation.

A restriction of PWP&EE is that, due to the low gradient of the sea floor, the closest a boat can approach the shore is a strong function of the tide. Furthermore, for the boats used in the trial, the closest available boat ramp was at Ardrossan requiring an approximate 25 km transit each way. The tide levels for the period of the trial are given in Appendix A.

Three transmission configurations were scheduled:

Land-to-land: Tx and Rx sites were at X4 and A2, respectively, at a distance of 1.14 km (Figure 2). This arrangement allowed both ends to be on land with the path of the laser beam over water except for a few metres across land on either end at high tide.

Shore-to-ship: The interrogator (Rx) was to be set up on the trial's boat, with the retro-reflector (Tx) on shore. However, this configuration was not able to be tested (Section 5.2), due to a forecast of unfavourable weather conditions.

Ship-to-shore: The optical interrogator (Rx) was set up at A2 (Figure 2) and the retro-reflector (Tx) was mounted on a tripod on the trial's boat. The closest range between Tx and Rx achievable was 1.92 km. This was due to depth constraints governed by the hull of the boat and sea depth from tide movements. The ranges used for testing the audio and video link were between 1.92 km and 3.8 km.

In order to characterise the atmosphere's effect on the FSOC links, measurements of atmospheric scintillation (Section 4.2.8) were taken using a commercial scintillometer (Scintec BLS 900). The transmit and receive ends were located at X4 and A2, respectively, with a transit path of 1.14 km (Figure 2). At high tide this path was almost entirely across water. The scintillometer was not set up on the initial day due to high wind conditions but was set up on each of the following days.

The exact timings of the trial vessel deployments were dependent upon prevailing sea and weather conditions. These were generally within three to four hours of the high tide (see Appendix A), depending on the size of the low tide.

Communication via two-way-radio was used between the Tx and Rx sites, provided by PWP&EE, and were regulated by the RSO (Range Safety Officer).

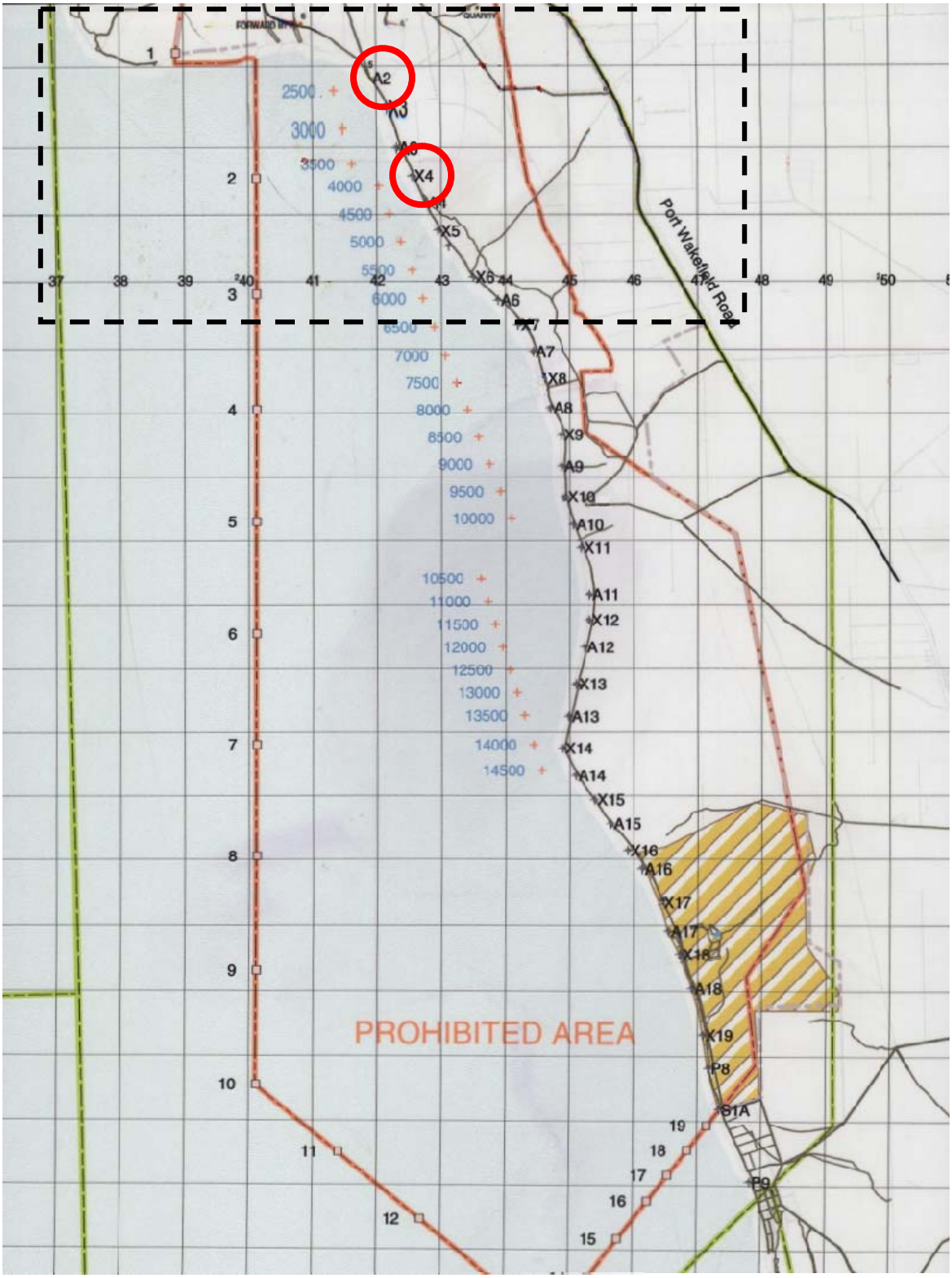

Figure 2 Port Wakefield P&EE, showing prohibited area. The squares are 1 km x 1 km. The inset is shown in Figure 20.

Figure 3: Satellite photo of area in map in Figure 2 ([9])

4.1 Safety

All hazards associated with the trial were identified and assessed as part of the trial planning process. A Risk Assessment (2114) using the Working Safer Tool was completed to determine likelihood and consequences of the hazards occurring and measures were developed to minimise these risks.

The laser beam's path was entirely confined within the prohibited area (Figure 2), by operating from site A2 and the forward battery and emitting the laser in approximately the north south direction. It was unconditionally safe to view the laser beam of this system with the unaided eye. However, the extended nominal ocular hazard distance (NOHDe – Appendix B) is the distance within which it is unsafe to view the laser beam with optical aids such as binoculars. Under worst case operating settings the NOHDe is 2.5 km. It is therefore possible to ensure that, outside the prohibited area, the laser beam poses no safety risk.

The Post Trail Safety report is found in Appendix C.

4.2 Equipment

The main equipment and components used in the trial are discussed in detail below.

4.2.1 Boats

The 10.5 m long boats used in this trial were the *Offshore Express* (Figure 4) and *M057 (*Figure 5*).* Due to the shallow water, the *Offshore Express* was severely limited as to how close it could approach the shore, and was only used on the first day of sea trials (21 September). The *M057* was subsequently used as its lower draft and outboard motor enabled it to get closer to shore and operate in lower tides. The equipment used for the FSOC link demonstrations was mounted on a tripod at the stern of the boat. To enable the boat to remain at a fixed range and as stationary as practical during the measurements, two anchors, situated at the bow and stern, were used.

Figure 4 Offshore Express

Figure 5 M057

4.2.2 Modulating Retro-reflector (MRR)

The operation of a FSOC link using a modulating retroreflector is schematically depicted in Figure 6. The figure shows the transmitted continuous wave interrogation beam, the electroabsorption amplitude modulator, and the retro-reflected beam that is amplitude modulated with the data and collected at the optical receiver. This technology has formed the basis of the US Navy's research and development program on asymmetric laser communications [11].

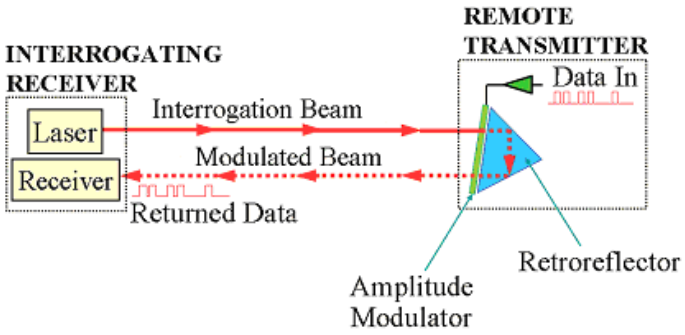

Figure 6 Operation of modulating retro-reflector

The electroabsorption modulator consists of multiple InGaAs coupled quantum-wells within the intrinsic region of a large area, *p-i-n* diode, designed to operate at a wavelength of 1.55 µm. The quantum-wells have the property that they alter their absorption with changing applied voltage. Hence, the device provides optical intensity modulation with an applied voltage data signal [10]. Details of the semiconductor design are given in Appendix D.

Figure 7 shows a packaged and mounted 6.3 mm diameter MRR. Included in the MRR package is a corner cube retroreflector and a buffer amplifier. The pictured MRR was loaned to DSTO by the US Naval Research Laboratory, as an equipment and material transfer (E&MT) under the auspices of TTCP SEN-TP-5. As MRR devices are not currently commercially available, DSTO has a research programme to fabricate and package these

devices and improve their modulation performance. Figure 8 is an image of the MRR mounted on a tripod, as it was used on the boat.

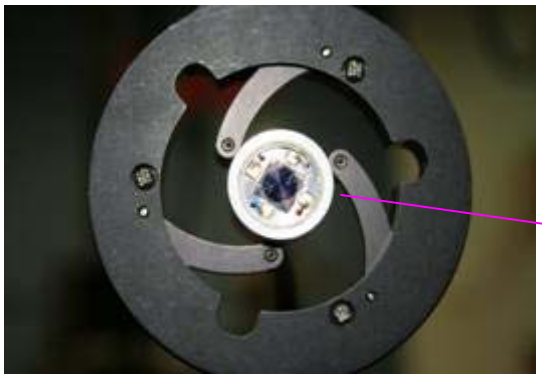

Figure 7 Close up of MRR

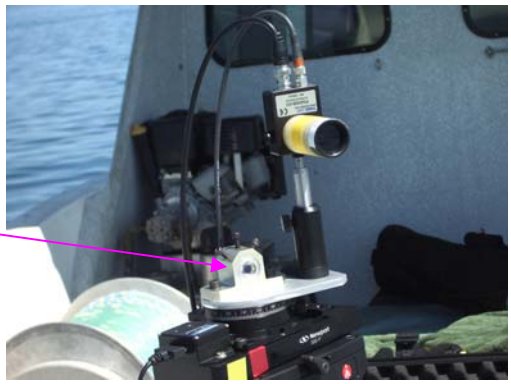

Figure 8 MRR mounted on tripod

To obtain the largest return signal practical from the MRR, the device is created with as large an area as possible, while maintaining the desired modulation bandwidth. Since the capacitance of the diode structure of the MRR increases with area, the MRR forms a first order RC filter whose cut-off frequency is:

$$f_{-3dB} = \frac{1}{2\pi RC} \tag{1}$$

where: f_{-3dB} = 3dB loss frequency of the lowpass RC filter [Hz]
R = output resistance of driver stage [Ω]
C = distributed capacitance of MRR's internal circuit and its connecting cable [F]

The capacitance of the MRR is estimated to be 500pF. From Appendix E the output resistance of the buffer amplifier used to drive the MRR is 3Ω. Thus f_{-3dB} is 10.6 MHz for the MRR, which is sufficient for the FM video system to operate at a carrier of 10 MHz, but causes attenuation to the upper FM sideband. Part of the DSTO research programme is to pixelate the MRR device and drive the pixels in parallel with separate amplifiers. This would increase the MRR bandwidth, producing better video quality.

The MRR, as provided by NRL, had a 360 mm length of miniature co-axial cable attached, which has associated with it a distributed capacitance to ground. This capacitance, together with the input capacitance of the MRR's internal electronics, combined with the output resistance of the driver used to deliver signals to the MRR also forms a RC filter. The distributed capacitance is fixed and is dictated by the length of co-axial supplied attached to the MRR and its internal electronics. A 360 mm length of miniature co-ax has a measured capacitance of 46pF, add to this an estimated gate capacitance of 30pF for the EL7202 buffer amplifier (Appendix E) which is built into the MRR gives an estimated 76pF for the value of C. Assuming a resistance R of 100Ω equation (1) yields a f_{-3dB} of 21 MHz. As this is significantly greater than the f_{-3dB} of the MRR and driver, it can be neglected as having an effect on the link's performance.

Figure 9 shows the MRR Driver circuit, which provides TTL input levels to the MRR's buffer amplifier. A 1N4004 steering diode is used to protect the +5 V voltage regulator from reverse polarity. The BFG235 transistor is biased to approximately ½ V_{cc} at the collector. The input signal drives the transistor into saturation and cut-off.

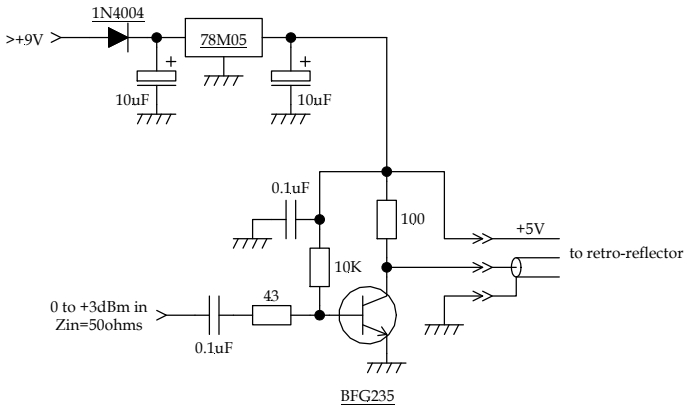

Figure 9 The MRR driver circuit

4.2.3 Interrogator

The interrogating receiver function of Figure 6 was performed by a NovaSol Compact Dual Mode Optical Interrogator (DMOI), shown in Figure 10. The dual modes of the DMOI are a retro-reflection mode, as was used in this trial, and a symmetric mode, where a DMOI is used at each end of the link. The NovaSol DMOI was developed in conjunction with the US Naval Research Labs, as part of their FSOC programme. The unit that was delivered to DSTO is export controlled and it was the first to be delivered outside the US.

The interrogator contains fibre coupled 100 mm diameter telescopes for transmit and receive functions. Each telescope also contains a fast steering mirror in the optical path, to perform pointing, acquisition and tracking, as schematically depicted in Figure 11. The fast steering mirrors are controlled by an internal DSP, whose actions are directed from software on a connected laptop. A sceeenshot of the software's interface is given in Figure 12. The software allows user control of the following operational parameters: transmitter beam divergence (50-2000 µrad); transmitter output power (0.5-2 W); scanning field of regard; and selection of internal or external optical detector.

The interrogator contains an internal erbium doped optical amplifier (EDFA) that boosts the (continuous wave or modulated) signal from an external seed laser source. The seed laser used in the trial was a NewFocus TLB3900 Tunable DWDM laser, set to a wavelength of 1.50 µm. This wavelength was selected so as to maximise the contrast ratio of the modulated signal from the MRR.

The receive telescope is coupled to a 100 µm core diameter multimode optical fibre. The receive fibre was connected to a pinfet photodetector (LDI, model LDPW-0012-105FCR). This model detector was chosen due to its high sensitivity and integrated automatic gain control circuit, which provides a large dynamic range that is necessary to cope with scintillation noise. Approximately 10% of the received light is directed, via a beam splitter,

to a quad detector. The quad detector is a position sensitive detector that is used to close the tracking feedback loop and maximise the light coupled to the multimode fibre.

To compensate for large movements, outside the dynamic range of the fast steering mirrors (such as might be expected from the motion of a boat), the interrogator was mounted on a tracking gimbal (Directed Perceptions, model PTU-D300). The gimbal operates on two axes and is able to cover 360˚ in azimuth and ±60° in altitude.

Figure 10 NovaSol Dual Mode Optical Interrogator

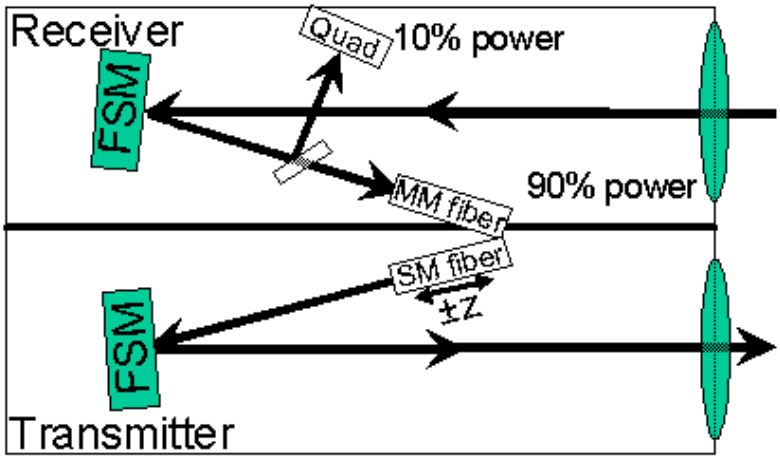

Figure 11 Schematic of interrogator

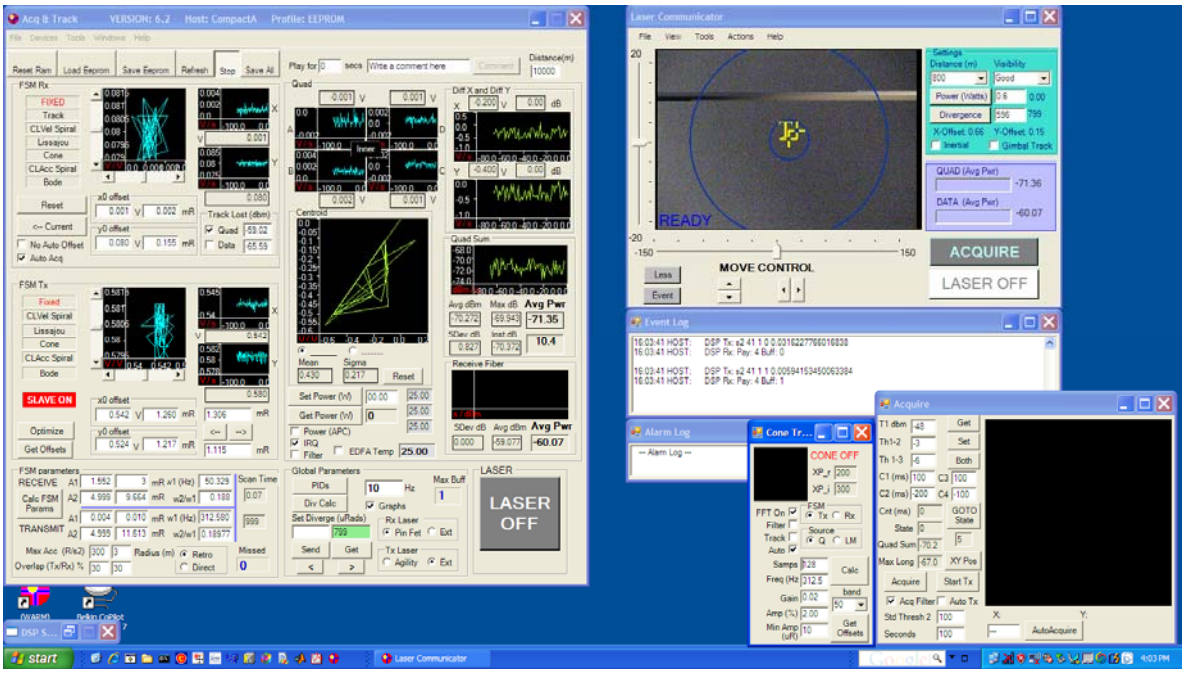

Figure 12 Screenshot of software interface for directing the interrogator. In the top right, video from a boresighted camera is shown. This is used to help initially acquire the target.

4.2.4 10 MHz Frequency modulator for audio/video

Effects arising from scintillation can be mitigated by the use of frequency modulation. This is because the data link is not affected by fluctuations in signal amplitude, except for a complete signal drop-out. In this case analogue FM modulation with a 10 MHz carrier frequency was used. The MRR was driven by the frequency modulated video signal, by either a live feed from a bullet camera or an audio/video output from a DVD player.

Figure 13 shows a block diagram of the FM modulator for audio/video, which was situated at the MRR end. A 5.5 MHz voltage controlled oscillator (VCO) has its frequency modulated by the audio input. This forms the audio sub-carrier which is then added via a resistive network to the video input. The combined video/audio sub-carrier then frequency modulates the 74 MHz VCO. The 74MHz FM signal is buffered and mixed with 64 MHz to produce 138 MHz and 10 MHz FM signals. The 138 MHz signal is filtered out by a 17.5 MHz low-pass filter. A 10.7 MHz low-pass filter couples the remaining 10 MHz FM signal to the optical modulator. This bandwidth is sufficient to support colour composite video. The circuit diagram for the 10 MHz FM receiver is shown in Appendix F.

Note that, in previous work, a 52 MHz local oscillator was used instead of the 74 MHz one [12]. This produced a 12 MHz modulated carrier when mixed with the 64MHz oscillator. This is above the MRR's 3dB frequency response range of 10 MHz. Furthermore, this modulation scheme caused the video synchronisation pulses to appear at the upper end of the modulated frequency spectrum where they were attenuated due to high frequency roll-off. Under conditions of high atmospheric scintillation, this resulted in tearing of the video image due to poor synchronisation. Using a 74 MHz VCO results in a 10 MHz modulated carrier, which minimises high frequency roll-off of the signal. Additionally, the

image tearing is reduced by the placement of the synchronisation pulses at the low frequency end of the modulated spectrum.

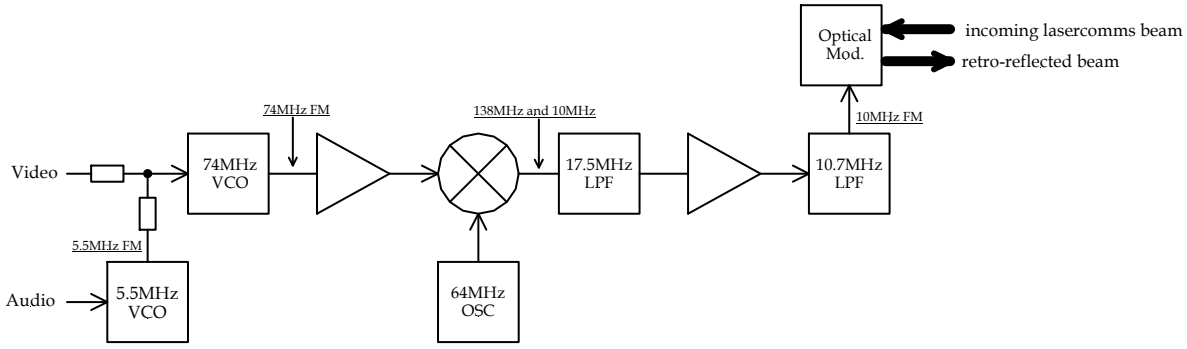

Figure 13 Block diagram of FM modulator for audio/ video

4.2.5 10 MHz Frequency demodulator for video

Figure 14 shows a block diagram of the frequency demodulator for analogue audio/video signals. This is located at the interrogator end of the link. The 10 MHz FM voltage signal output from the optical detector (LDI, pinfet model LDPW-0012) was mixed with a 490 MHz sine wave to produce 480 MHz and 500 MHz FM signals. These signals, which have varying amplitude caused by atmospheric scintillation were fed to the input of the receive module where only the 480 MHz FM signal was processed. The 480 MHz FM receiver/demodulator module was a modified commercially available satellite receiver (Racewood Secu-Tech, model CCTV-1200TR-1500) in order to make use of its in-built 480 MHz bandpass filter, FM receiver with limiter, and an FM video demodulator with audio sub-carrier demodulation. The FM receiver's IF stages progressively amplify the 480 MHz sine wave amplitude varying signal to such an extent that it over drives the last stage (the limiter). This results in a square wave signal produced at the limiter's output whose envelope is constant in magnitude and varies in frequency corresponding to the FM input. This constant magnitude FM square wave was FM de-modulated to recover the video and audio sub-carrier. The audio sub-carrier was further FM demodulated to recover the audio (MiniKits, model EME158 KIT1). The output from the receiver module was fed to the input of a LCD monitor for viewing or to a laptop for recording via a video capture card (Matrox, model MXO2mini).

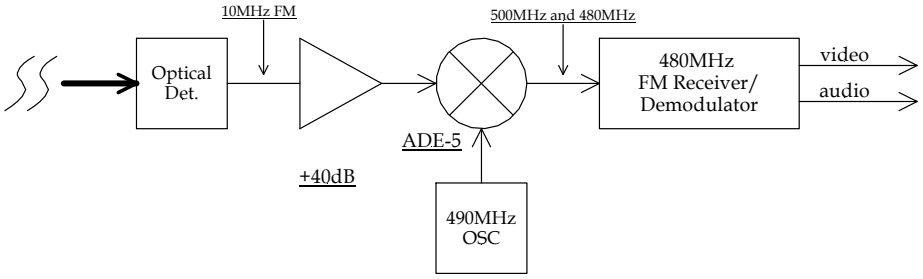

Figure 14 Block diagram of FM demodulator for video

4.2.6 Audio 60 kHz FM Modulator

As shown in Figure 6, the standard operation of an MRR communications link is to use a continuous wave optical interrogation beam. However, this only allows the transmission of information from the MRR back to the interrogator. In the current work, a novel method was developed to enable duplex communications, by using an interrogation beam modulated with a low depth of modulation data signal, detected at the MRR end of the link using a separate optical receiver. To this end, the outgoing laser beam was amplitude modulated with a 60 kHz carrier. The carrier was then frequency modulated with an audio signal. However, as the MRR is a non-linear device that heterodynes the 60 kHz carrier with the 10 MHz video signal, resultant cross-products are seen as artefacts in the demodulated video. Laboratory measurements before the trial showed that modulation depths of up to 6% could be used. Beyond that, the level of the induced artefacts was unacceptable.

This technique could also be applicable in future applications, such as the transmission of a control signal to an unattended sensor, or as part of an error correction system to request the MRR to resend data.

4.2.7 Audio 60 kHz FM Demodulator

The audio photoreceiver (right hand side of Figure 8) was mounted approximately 100 mm from the MRR in order that they would be in the interrogating beam simultaneously. A COTS 5mm diameter germanium photodetector (Thorlabs, model PDA50B-EC) with switchable gain (0 to 70dB in 10dB steps) was used to detect the laser beam. This is sensitive in the region 800 to 1800 nm, with a responsivity of approximately 0.85A/W at 1550 nm. A compound parabolic concentrator (Edmund Optics, model NT65-442) was mounted in front of the photodetector. Its 18mm input diameter gave approximately 10dB of gain over using the bare detector. Furthermore, it has a ±25° acceptance cone, which compares favourably with an f/1 lens of the same diameter that has a field-of-view of ±8°. An optical bandpass filter (Edmund Optics, model NT65-793, 1550 nm centre wavelength, 12 nm width) was used to minimise the amount of ambient light being detected.

The 60 kHz FM receiver (Figure 15) was designed with a very high input impedance so that it could be connected directly to a photodiode. This high input impedance was made compatible with the COTS detector by fitting an external 50 ohm termination to the input

of the receiver and the internal gain of the COTS photodiode detector was compensated for by installing an input attenuator.

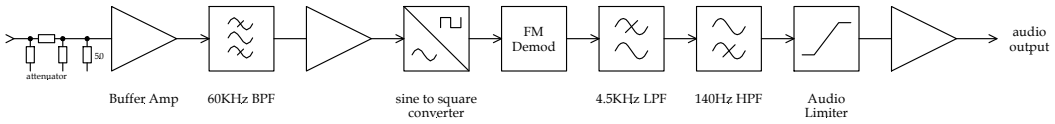

Figure 15 Block diagram of 60 kHz audio receiver

The 60 kHz bandpass filter is an active design in which a series resonant circuit is used to control the gain of a common emitter transistor (Figure F-1). The bandwidth is controlled by the choice of L/C ratio in conjunction with the emitter resistor. The output of the filter drives the main gain stage.

Three op-amps provide the main stage gain. The gain was chosen so that, in the absence of an optical input signal, the broadband noise generated by the input buffer stage was just sufficient to drive the sine to square wave converter into saturation and cut-off. This ensures that the minimum optical signal triggers the FM detector, resulting in maximum sensitivity without introducing significant non-linear distortion.

Most FM demodulators are sensitive to amplitude variations in their input signals as well as the frequency. The sine to square wave converter is used as a limiter to remove any amplitude variations in the 60 kHz signal before it is coupled to the FM demodulator. The limiter is an open loop gain op-amp whose output connects directly to the FM demodulator.

The 60 kHz FM demodulator is of the pulse count discriminator type. A charge is built-up in a capacitor during the positive duration of the signal and the capacitor is discharged through a resistor during the negative duration. The voltage developed across the discharge resistor is calculated by:

$$V = V_p \, f \, RC \tag{2}$$

where: V = voltage developed across R (V)
V_p = peak signal voltage (V)
f = frequency (Hz)
R = 6K8 = discharge resistor (ohms)
C = 1.33nF = charging capacitor (F)

A 10 nF filter capacitor connected from R to ground smooths out the 60 kHz component producing the demodulated audio.

Two op-amps are used as high and lowpass active audio filters to band limit the range of frequencies appearing at the output of the FM demodulator. The 140 Hz highpass helps to control the sound of the wind blowing across a microphone. The 4.5 kHz lowpass limits the audio upper frequencies to the accepted communication range and also helps to suppress the high frequency hiss.

The bandwidth of the 60 kHz bandpass filter is much greater than the +/-10 kHz maximum deviation of a received modulated 60 kHz signal. At times of deep fades due to atmospheric scintillation, the full bandwidth of noise in the 60 kHz filter is applied to the FM demodulator giving rise to a demodulated audio signal whose magnitude is many times greater than the +/-10 kHz limited deviation of the wanted signal. This large increase in audio volume from a wanted audio signal to broadband noise in the frequency range of 140 Hz to 4.5 kHz has its magnitude controlled by an audio limiter installed directly after the audio filters. The circuit diagram of the 60 kHz receiver is shown in Appendix F.

4.2.8 Scintillometer

Atmospheric turbulence is typically measured in terms of the refractive index structure parameter, C_n^2. As shown schematically in Figure 16, temperature variations induce changes in the refractive index in air, causing fluctuations in the amplitude and phase of a laser beam as it propagates through the atmosphere. [1] (This is the same phenomenon that causes the twinkling of a star.)

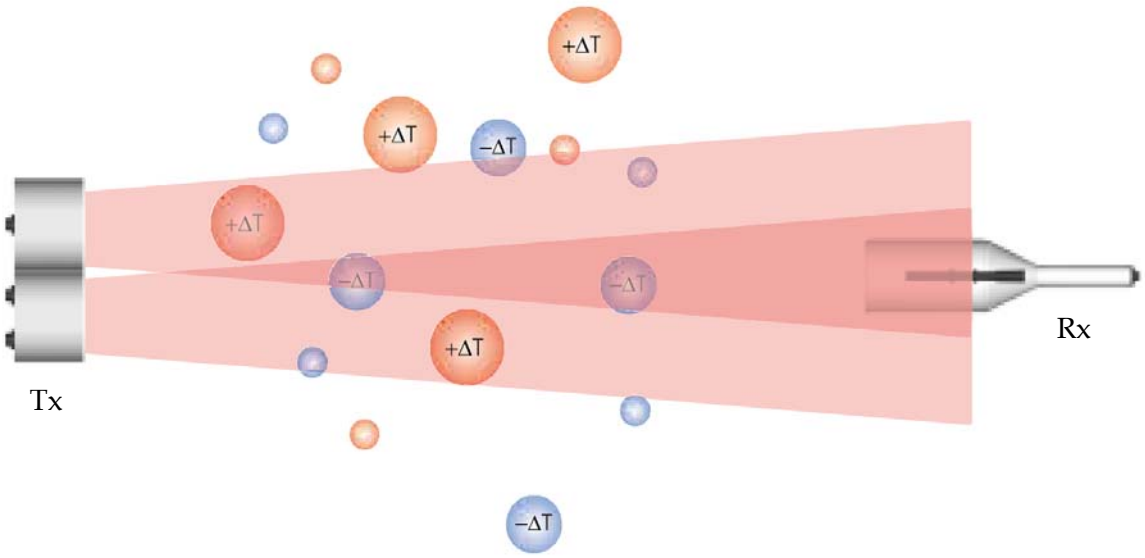

Figure 16 Refractive index fluctuations induced by thermal turbulence cause the received intensity to fluctuate [4]

A commercial scintillometer (Scintec, model BLS900) was used to measure and record C_n^2 at 1-minute intervals. The BLS900 consists of a transmitter (Figure 17) and receiver (Figure 18), located up to 5 km apart. The transmitter contains two disk-shaped arrays of 450 light emitting diodes (LEDs). The BLS900 estimates C_n^2 evaluating the variance of the intensity fluctuations at its receiver.

Figure 17 BLS900 transmitter

Figure 18 BLS900 receiver

Specifications of the BLS900 are shown in Appendix G.

Representative median values of C_n^2 are 10^{-14} $m^{-2/3}$ [14] and 10^{-13} $m^{-2/3}$ in the maritime and terrestrial environments, respectively [15]. This is due to the difference in temperature gradients above water compared with that above land.

The purpose of measuring the atmospheric scintillation was to compare the link quality and degradation with the C_n^2 value. Ideally, C_n^2 would be measured along the same propagation path as the communication channel. This was not possible in the present case, as both ends of the scintillometer need to be completely stationary during the measurement, which is not possible with a boat at one end of the link. Thus, the C_n^2 values measured should be considered indicative of those of the communications link rather than definitive.

4.2.9 DC power supply

In order to obviate the safety issues inherent in using mains power in a maritime environment, power for the shipboard part of the experiment was derived from two 12V, 75Ah deep cycle sealed lead acid batteries. These two batteries were connected in series providing the required 24V. Various voltages were required by the different pieces of equipment drawing its power from these batteries (Figure 19). DC-to-DC switch mode converters were employed to minimise power wasted through the generation of heat when converting voltage levels, which maximises the time between battery charges. A fused battery distribution box was constructed which allowed quick connection and disconnection of various pieces of equipment depending upon the experiment being carried out at the time.

Gold plated hermetically sealed military grade DC-to-DC converters supplied by VPT-Inc. (USA) were used. The gold plating and hermetic sealing was needed to combat salt induced corrosion from sea spray. As DC-to-DC converters are notorious generators of unwanted electromagnetic fields, the various converter modules used were all fully enclosed in a metal shield restricting their EMI emission. Special EMI filters were also fitted between the long battery lead and the converter to minimise unwanted RF radiation from the leads.

The Dell laptop computer used to drive the interrogator posed a problem when being powered from an external source of DC power, as a result of a proprietary chip contained within Dell plug packs identifying compatibility with the laptop. To circumvent this, a compatible chip was wired into the cable between the DC-to-DC converter and the laptop.

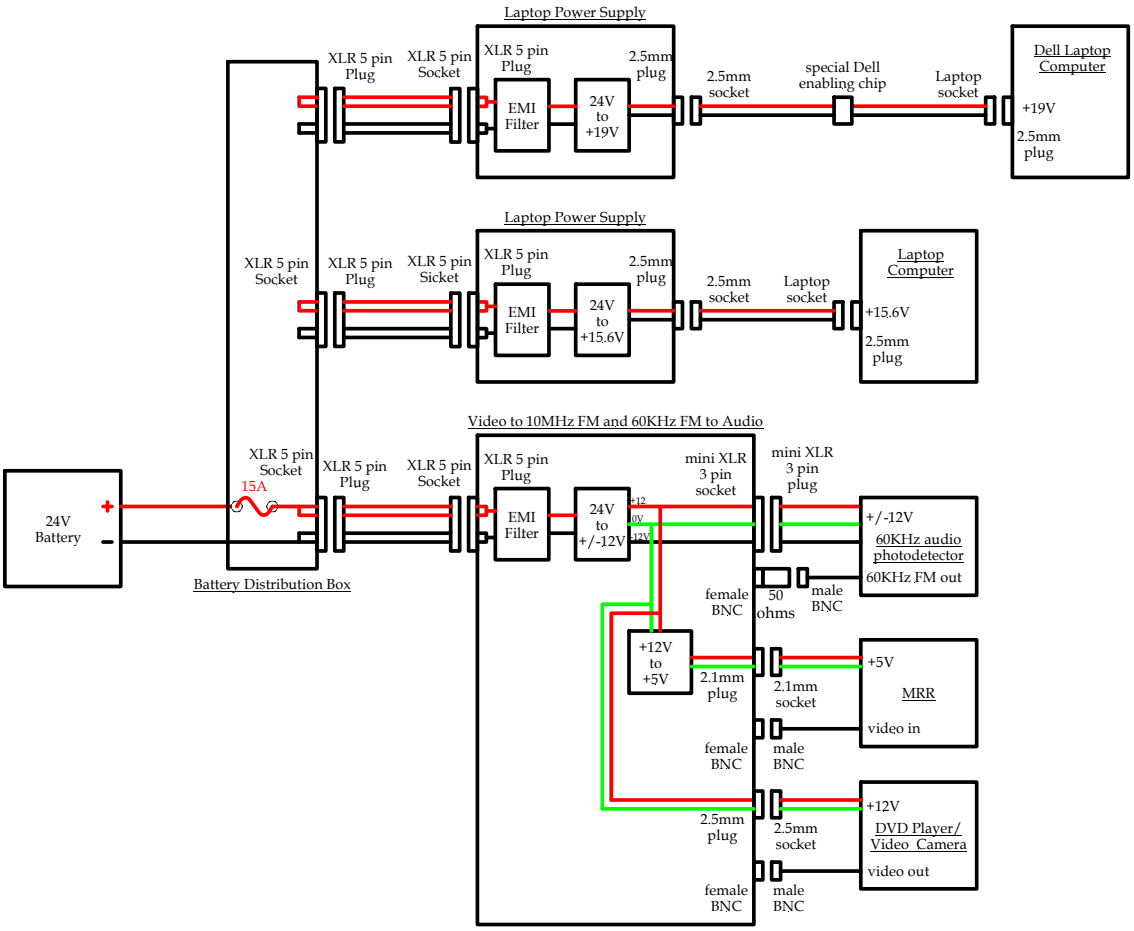

Figure 19 DC power supplies for shipboard equipment

5. Results

In this Section, the experiments and optical link demonstrations that were performed on each day of the trial are discussed. The tests were largely conducted according to the schedule proposed in the trial plan (Maritime Laser Communications Trial 98152-19703) but were modified due to safety considerations, as appropriate, in cases of unfavourable weather conditions.

5.1 Equipment test onshore – Monday, 19 September, 2011

The primary objective on the first day was to test equipment in a land-to-land configuration at the trial site to demonstrate all equipment was working correctly and that an optical link could be closed. Before being given access to the range, a safety briefing and instructions on radio communications protocol was given by Port Wakefield P&EE staff.

Transmit and receive sites were set up on the shore near sites A2 and X4, respectively, as shown in Figure 20. This allowed both ends of the link to be set-up on land but with the laser beam path largely across water at high tide.

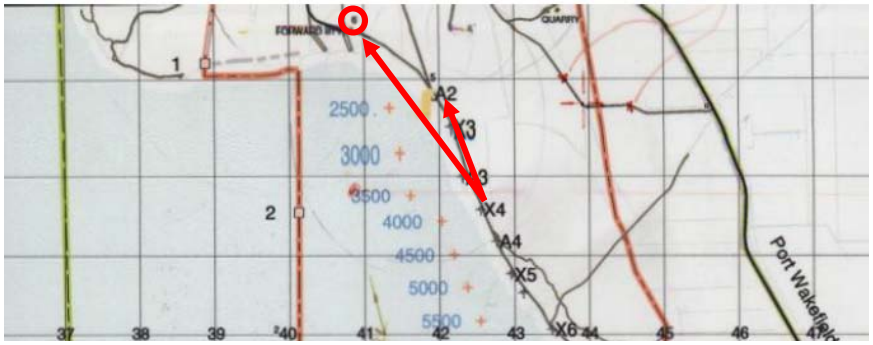

Figure 20 Inset of Figure 2 showing the optical link locations. The squares are 1 km x 1 km.

Very high winds were experienced on the first day which meant it was not practical to set-up the scintillometer. However, the optical link equipment was shown to be operating correctly.

5.2 Shore-to-shore link across water –Tuesday, 20 September, 2011

A shore-to-ship link was originally scheduled for 20 September in which the optical interrogator is mounted on a tripod on the boat with the MRR located on shore. Unfortunately, a forecast of high winds prevented the boat from being launched due to safety considerations. Due to time constraints and further unfavourable weather conditions (Appendix H), this configuration was unable to be tested on the trial.

Instead, further tests of shore-to-shore communications across water were conducted at varying ranges. Ranges were measured using way point locations determined by GPS units (Appendix I). The interrogator was initially set up in an instrumentation van at the Forward Battery (FB) (Figure 21), with the MRR and audio receiver mounted on the rear of a Unimog at position X4 (Figure 22). The locations are shown in Figure 20 and correspond to a range of 2.4 km. The beam height was approximately 2.5m. During this period C_n^2 was approximately $6x10^{-14}m^{-2/3}$.

Figure 21 Interrogator in the instrumentation van. Scintillometer receiver at right.

Figure 22 MRR and audio receiver on the Unimog. Scintillometer transmitter at lower left.

The interrogator was able to locate the MRR and maintain lock on it. Useable video (although with occasional drop outs) and good two-way audio transmission were established. (A "useable" video link is one that is largely free from artefacts and noise caused by link drop-outs, with a clear image.) Figure 23 shows a frame from the captured video at a distance of 2.4 km. Optical power was 1.6 W and beam divergence was 180 μrad.

Figure 23 Captured video frame at 2.4 km

The interrogator was subsequently moved to site A2, giving a range of 1.15 km to the MRR location at X4 (Figure 20). Good quality video and audio were achieved with an optical output power of 500 mW and 400 μrad divergence. Table 2 summarises the results for 20 September.

Table 2: Shore-to-shore results for 20 September

Location	**Distance [km]**	**Power [W]**	**Divergence [μrad]**	**Cn^2 [$m^{-2/3}$]**	**Audio**	**Video**
X4 to FB	2.4	1.6	150	$6x10^{-14}$	✓	✓
X4 to A2	1.15	0.6	400	unknown	✓	✓

5.3 Ship-to-shore link – 21-23 September, 2011

In this Section, results for the ship-to-shore links are presented. In this configuration the interrogator was located on shore at position A2 (see Figure 20) transmitting to the MRR mounted on a tripod on a boat. The ship-to-shore links were tested on Wednesday, 21 September to Friday, 23 September inclusive. The optical scintillometer was set-up between the interrogator location at A2 and the position X4 each day, to monitor the atmospheric turbulence level. As a result the scintillometer beam path is not co-located with the optical link path and therefore the measured C_n^2 values are considered representative only.

5.3.1 Wednesday, 21 September

The weather conditions were fine, with light wind and sunny conditions. The boat used was the *Offshore Express* which was anchored at varying ranges from the interrogator location at A2, starting at the closest range achievable and progressively moving further out. The closest range was determined by the tide height and draft of the boat and was approximately 2.3 km. Table 3 below displays the results for the optical links and C_n^2 for each transmission distance.

Table 3: Ship-to-shore results on 21 September

Distance [km]	**Power [W]**	**Divergence [μrad]**	**C_n^2 [$m^{-2/3}$]**	**Audio**	**Video**
2.26	1.6	200	10^{-13}	✓	✓
3.07	1.6	150	10^{-13}	✓	✓
3.7	1.6	150	$2*10^{-13}$	✓	×

At a distance of 2.26 km the video was good quality with minimal artefacts even with a high C_n^2 value of 10^{-13} $m^{-2/3}$. The maximum link distance achieved for both a useable video audio link was at 3.07 km. This corresponds to 1.66 nautical miles and a C_n^2 value of 10^{-13} $m^{-2/3}$..

At 3.7 km, a link was established and tracked by the interrogator but only a bidirectional audio link was achieved. The factors contributing to the inability of establishing a video link were scintillation and insufficient transit power. In this case the interrogator was transmitting at its maximum power of 1.6W and a divergence of 150μrad.

The slow gradient of the sea floor at the Port Wakefield proof range site results in a large distance between the high and low water marks. This varies with tide heights and wind conditions but is typically of the order of several hundred metres. As a consequence proportionally more of the laser beam path traversed over tidal flats rather than over water as the tide went out during the course of the measurements. This results in less favourable atmospheric conditions as the scintillation is typically higher over land than water.

5.3.2 Thursday, 22 September

Very high winds were experienced on Thursday and as a result the boat was not able to be effectively anchored in position without the anchor dragging during optical link tests. Furthermore, significant sea spray on the MRR, particularly during boat anchoring, required it to be periodically cleaned or covered up as a result. Consequently there were limited opportunities available to perform the optical link tests. The results of 22 September are summarised in Table 4.

Table 4 Ship-to-shore results on 22 September

Distance [km]	**Power [W]**	**Divergence [μrad]**	**C_n^2 [$m^{-2/3}$]**	**Audio**	**Video**	**Comments**
3.8	1.6	150	5 to 12 x 10^{-14}	×	×	Difficulty holding track on passive retro
3.2	1.6	150	5 to 12 x10^{-14}	×	×	Would hold track on passive retro but not MRR
2.3	1.6	150	5 to 12 x 10^{-14}	Audio out OK, returned audio marginal	×	Would hold track on MRR

The interrogator was not able to close a video link, even though the C_n^2 value in each instance was lower than that for the high quality video obtained on 21 September. This was due to the very high wind speed which resulted in much more boat pitch and roll as well as the difficulty encountered in anchoring the boat effectively in these weather conditions. Accelerometer measurements of the boat movement at anchor on the respective days are shown in Appendix J

Due to high winds (~25 knots) the boat had to return to harbour at 1000 and trial activities ceased for the day.

5.3.3 Friday, 23 September

The weather on this day was fair, with moderate wind speeds. Both an audio and video link were achieved, maintained and tracked. The video was of useable quality, although it lost synchronisation occasionally due to signal drop outs. However, the audio signal was of good quality but included some "pops". Results are summarised in Table 5.

Table 5 Ship-to-shore results on 23 September

Distance [km]	**Power [W]**	**Divergence [μrad]**	**C_n^2 [$m^{-2/3}$]**	**Audio**	**Video**
2.2	1.6	150	1x10^{-13}	✓	×

A demonstration of the FSOC system was given to Navy Communications and Information Warfare Branch staff. Of significant interest to the Naval personnel was the

high quality of the audio, which far surpassed the audio quality from the UHF radios that were in use for the trial.

6. Summary and Future Work

An eye-safe, free space optical communications link over water at a transmission distance of 3.07 km was successfully demonstrated. These measurements indicate that this FSOC system can provide additional capability for the RAN, particularly during EMCON conditions. Further, it has the potential to be extended to ship-to-ship communications.

The following trial aims were achieved:

- Land-to-land FSOC demonstration across water

  Video and bidirectional audio were successfully transmitted land-to-land across water at ranges up to 2.4 km

- Testing of NovaSol optical interrogator on shore to track a retro-reflector on a boat

  The interrogator was able to track a passive retro-reflector at a range of 3.7 km

- Testing of novel FM audio/video communication system at different ranges

  To our knowledge this is the first demonstration of a bidirectional audio/video link using MRRs. Indeed, once the link was established the laser audio link was preferred to the two-way radio link.

- Testing the ability to maintain a ship-to-shore lasercomm link at different ranges

  The link was closed over ranges from 2.2 to 3.7 km

The aims of the trial not fully achieved were:

- A video and audio link at a range of two nautical miles, or 3.7 km

  Although a video link was not established at 3.7 km, an audio link was successfully demonstrated

- Testing the NovaSol optical interrogator on a boat to track a retro-reflector on shore

  Due to weather conditions and time constraints it was not possible to test the interrogator on board the boat

Future work will include:

- Adapt the current analogue FM communication system to digital data. Research is currently underway with the University of South Australia to develop forward error correction coding to enable the link to cope with data loss from deep signal fades.

- Continue development of in-house fabrication of MRR devices, including the implementation of simulated improvements to the NRL design [16]. To increase the available link range and/or immunity to drop outs caused by the atmospheric scintillation noise, an array of multiple MRR devices will be fabricated.

- Investigation of symmetric links (using a pair of interrogators) in the maritime environment. This would involve continuing development of an in-house optical tracking interrogator or the purchase of a second commercially available interrogator. Symmetric links allow for substantial increase in the link range and data rates achievable at the expense of system complexity and cost.

- Investigation of the internal tracking system of the NovaSol interrogator, to determine whether the tracking system was misaligned. This would present an explanation of the inability to close a link on 22 September.

- The current test of video quality is subjective. Techniques will be investigated to quantitatively characterise the system.

- It is not possible to draw firm conclusions as to the performance of the system with respect to C_n^2, as measurements were made over different ranges and on different days with varying meteorological conditions. This was further complicated by the possibility of misalignment within the receiver module of the interrogator. This is the subject of further investigation.

- Measurements obtained before the trial indicated that the MRR has a field-of-view of approximately 45 degrees. In the current trial, due to the movement of the boat at anchor, the MRR had to be manually realigned to point towards the interrogator (on a time scale from ~10 seconds to a few minutes). An MRR array, instead of a single MRR, is a possible solution to increase the FOV of the MRR to 360 degrees, thus eliminating the need to manually rotate it to maintain tracking.

7. Acknowledgements

The authors gratefully acknowledge: financial support from the Navy Communications and Information Warfare Branch; trial safety and logistical support from Samantha Carter; and the assistance of Wayne Nagle and Les Badari in the running of the trial.

8. References

[1]. Andrews, L. C. and Phillips, R. L., (2005), *Laser Beam Propagation through Random Media*, SPIE Press

[2]. Santanu Das, Hennes Henniger, Bernhard Epple, Chrisopher I. Moore, William Rabinovich, Raymond Sova and David Young, *Requirements and Challenges for Tactical Free-Space Lasercomm,* IEEE Military Communications Conference, Nov 2008

[3]. Moore, C.I., Burris, H.R., Rabinovich, W.S., Suite, M.,Wasiczko L., Jarmeko, J., Ibanez, J., Georges, E. S. Uecke, S., Mock, J., Muth, J. F., Wood, T. S., *Lasercomm demonstration during US Navy Trident Warrier 06 Forcenet exercise,* IEEE Antennas and Propagation Society International Symposium 2007, pp 17-20

[4]. Juarez, J. C., Sluz, J.E., Nelson, C., Davidson, F. M., Young, D. W., Sova, R. M. *Lasercomm demonstration in a maritime environment for tactical applications,* OSA/ASSP/LACSEA/LS&C, 2010

[5]. Scott, R. *Beaming data: laser opens new paths to high-bandwidth communications at sea,* Janes International Defence Review, Nov. 2010

[6]. Kenneth J. Grant, James Murphy, Rita Mahon, Harris R. Burris, William S. Rabinovich, Christopher I. Moore, Linda M. Wasiczko, Peter G. Goetz, Michele Suite, Mike S. Ferraro, G. Charmaine Gilbreath, Bradley A. Clare, Kerry A. Mudge, Jason Chaffey, *Free Space Optical Transmission of AM composite Video Signals Using InGaAs Modulating Retro-reflectors,* Conference on Optoelectronic and Microelectronic Materials and Devices, 2006

[7]. K.J. Grant, B.A. Clare, W. Martinsen, K.A. Mudge, H.R. Burris, C. I. Moore, J. Overfield, G. C. Gilbreath, W. S. Rabinovich and J. Duperre, *Laser Communication of FM Audio/Video Signals Using InGaAs Modulating Retro-reflectors, Proc. of SPIE vol. 8038, 80380K-1, 2011*

[8]. H.R. Burris, F. Bucholtz, C.I. Moore, K.J. Grant, M.R. Suite, C.S. McDermitt, B.A. Clare, R. Mahon, W. Martinsen, M. Ferraro, R. Sawday, B. Xu, C. Fony, L.M. Thomas, K.A. Mudge, W.S. Rabinovich, G.C. Gilbreath, W. Scharpf, E. Saint-Georges, S. Uecke, *Long range, analog RF free space optical communication link in a maritime environment, Proc. of SPIE vol. 7324, 73240G-1, 2009*

[9]. maps.google.com.au [accessed March 2012]

[10].Stievater, T. H., Rabinovich, W. S., Goetz, P. G., Mahon, R., Binari, S. C., *A surface-normal coupled-quantum-well modulator at 1.55 micrometers*, IEEE Photonics Technology Letters, Vol. 16, 9, 2004, pp 2036-2038

[11].Rabinovich, W. S., Mahon, R., Burris, H. R., Gilbreath, G. C., Goetz, P. G., Moore, C. I., Stell, M. F., Vilcheck, M. J., Witkowsky, J. L., Swingen, L., Suite, M. R., Oh, E., Koplow, J., *Free-space optical communications link at 1550 nm using multiple-quantum-well*

modulating retroreflectors in a marine environment, Optical Engineering, Vol. 44, 5, 2005, pp 1-12

[12]. K.J. Grant, B.A. Clare, W. Martinsen, K.A. Mudge, H.R. Burris, C.I. Moore, J. Overfield, G.C. Gilbreath and W.S. Rabinovich, *Free Space Optical Transmission of FM Audio/Video Signals Using InGaAs Modulating Retro-reflectors*, Conference on Optoelectronic and Microelectronic Materials and Devices, Canberra Dec 2010

[13]. http:// www.scintec.com/PDFs/01_LayBLS.pdf [accessed March 2012].

[14].Thomas, L. M. W., Moore, C. I., Burris, H. R., Suite, M., Walter Reed Smith, J., Rabinovich, W., *NRL's research at the Lasercomm Test Facility: characterization of the maritime atmosphere and initial results in analog FM lasercomm*, Proc. 2008, Vol. 6951, pp 69510S

[15].K.A. Mudge, B.A. Clare and K.J. Grant, unpublished work

[16].B.A. Clare, K.A. Mudge, K.J. Grant, *Design of a Coupled Quantum Well Modulator with Enhanced Modulation Efficiency*, Proc. IQEC/CLEO Pac. Rim, Sydney, August 2011

Appendix A: Port Wakefield Tide Levels

PORT WAKEFIELD TIDE TIMES AND HEIGHTS: help Height: m

Mon Sep 19		Tue Sep 20		Wed Sep 21		Thu Sep 22		Fri Sep 23	
Low	12:22am 0.5 m	Low	12:38am 0.5 m	Low	12:56am 0.6 m	Low	1:04am 0.9 m	High	2:24pm 1.7 m
High	6:50am 2.4 m	High	7:14am 2.3 m	High	7:42am 2.2 m	High	8:15am 1.9 m	Low	9:39pm 0.8 m
Low	1:09pm 0.6 m	Low	1:35pm 0.7 m	Low	2:10pm 0.9 m	Low	11:22pm 1 m	-	- -
High	6:50pm 1.9 m	High	7:10pm 1.7 m	High	7:26pm 1.5 m	-	- -	-	- -

Figure A-1 Tide times for Pt. Wakefield during the period of the trial

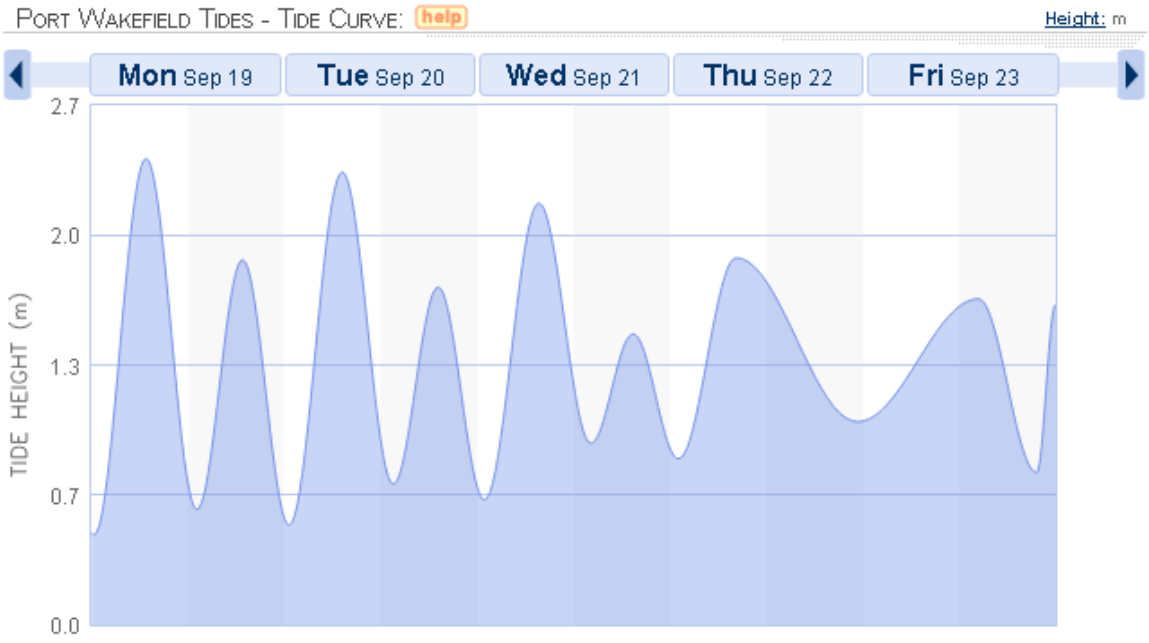

Figure A-2 Graphical representation of the tide level variation throughout the trial period

Appendix B: Laser Safety Calculations

In the current system, the wavelength is 1550 nm, maximum optical power output is 1.6W, the divergence is adjustable with a minimum of 0.1 mrad, and exit beam diameter (1/e) is 68 mm.

From Australian / New Zealand Standard 2211.1:2004 *Safety of laser products. Part 1: Equipment classification, requirements, and user's guide*, this laser system has a classification of 1M. This standard defines 1M lasers as those "emitting in the wavelength range from 302.5 nm to 4000 nm which are safe under reasonably foreseeable conditions of operation, but may be hazardous if the user employs optics within the beam." The output of a Class 1M laser is potentially hazardous when viewed using an optical instrument e.g. binoculars.

The nominal ocular hazard distance (NOHD) represents that range at which, under ideal conditions, the irradiance and the radiant exposure fall below the appropriate maximum permitted exposure (MPE).

According to ANZS 2211.1:2004, the NOHD is given by:

$$NOHD = ((4P_o / \pi.E_{MPE})^{1/2} - a) / \varphi$$

where P_o is the transmitted optical power,
E_{MPE} is the appropriate maximum permissible exposure ($10^3 W/m^2$),
a is the diameter of the emergent laser beam, and
φ is the divergence angle of the emergent laser beam.

Substitution of the appropriate values into this equation (using *LaserSafe PC* V4.02) yields an NOHD of zero metres i.e. the laser is eye-safe to the unaided eye.

The extended NOHD (NOHDe) takes into account the effect of using an optical instrument such as binoculars in the laser beam. In that case, the increase in the amount of radiation entering the eye is given by:

$$(\text{diameter of objective lens of viewing aid} / \text{theoretical pupillary diameter})^2$$

ANZS 2211.1:2004 takes the pupil diameter to be 7 mm, and the objective lens diameter to be 50 mm. Taking these factors into account yields NOHDe = 2.483 km.

Note that this value of NOHDe is the worst case scenario, and can be reduced by using lower laser power or increasing the beam divergence. For example, operating with the minimum laser power of 0.5W (with divergence 0.1mrad) yields an NOHDe of 1.088 km. These values of NOHDe are shown below in Figure B-1.

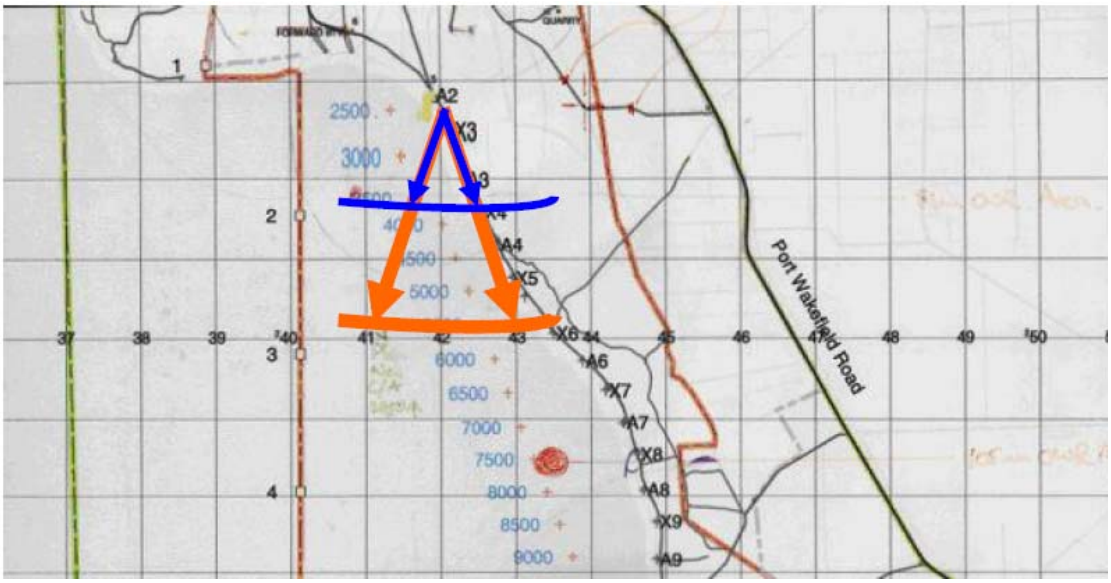

Figure B-1 Wakefield P&EE range, showing NOHDe at 200 mrad divergence

Appendix C: Post Trial Safety Report

Australian Government
Department of Defence
Defence Science and
Technology Organisation

Laser Communications Trial, Port Wakefield
As Per Risk Assessment No 2114

C3ID

Post Trial Safety Report

1. Introduction

This safety report covers the safety aspects for the Laser Communications, Port Wakefield trial, conducted between Monday 19th October, 2011 and Friday 23rd October, 2011.

2. Major Safety Issues/Incidents

No major incidences occurred during the trial that could have led to serious injury to personnel.

3. Minor Safety Issues/Incidents

No minor safety issues or incidents occurred.

4. Staffing and Training

In the months leading up to the trial, the trial participants undertook a course in Manual Handling.

Immediately prior to the trial, Mr Wayne Nagle, Operations Co Ordination Officer
Joint Proof and Experimental Unit, Proof and Experimental Establishment Port Wakefield delivered a safety brief. In addition, prior to boarding the boat, a safety brief was given by Mr Les Badari that included location of safety provisions aboard the boat and instructions on what to do in the event of an emergency. A pilot was provided to the boat by the Port Wakefield Proof and Experimental Establishment, as per their SOP.

5. Medical Clearance

All DSTO personnel who participated in the Trial completed two Emergency Information Forms – sealed in envelopes and placed within the First Aid boxes. One box was located at the land base within the truck and the other was located in the boat. The use of two emergency forms was because boat crew were expected to change with the land crew during the week and this was to avoid an occurrence of the emergency form being at the wrong location.

6. Protective equipment

Protective equipment was worn throughout the trial in accordance with the requirements of the trials/safety plan.

7. Conclusions/Recommendations

DSTO personnel on the trial followed the requirements as set out in the Safety section of the Trial Plan and in accordance with Risk Assessment Report No 2114. The trial was completed safely.

Appendix D: Modulator Design

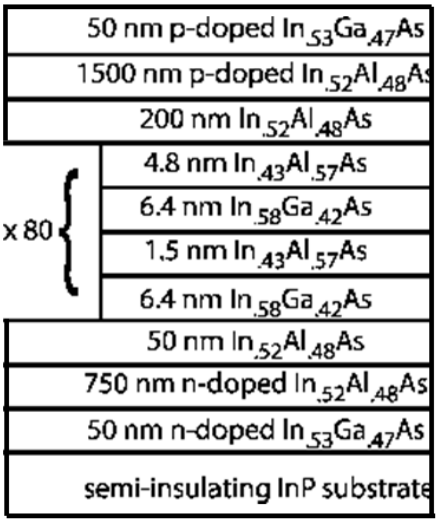

Figure D-1 Design of semiconductor layer structure used to create a multiple coupled quantum well electroabsorption modulator at 1.5 μm. This design is from [10].

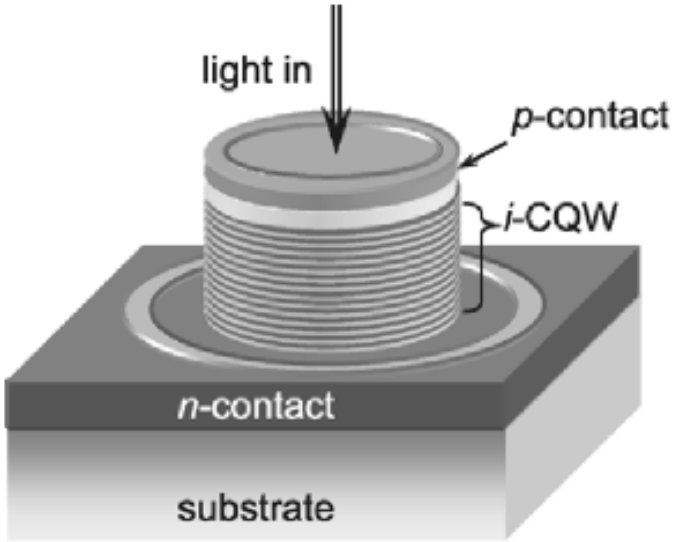

Figure D-2 Schematic diagram of the diode structure that embeds the electroabsorption modulator [10]. Note that the diagram is not to scale. The diameter of the modulator is ~6 mm and the height is ~4 μm.

Appendix E: EL7202 Data Sheet

intersil

EL7202, EL7212, EL7222

Data Sheet | **May 9, 2005** | **FN7282.1**

High Speed, Dual Channel Power MOSFET Drivers

The EL7202/EL7212/EL7222 ICs are matched dual-drivers that improve the operation of the industry standard DS0026 clock drivers. The Elantec versions are very high speed drivers capable of delivering peak currents of 2.0 amps into highly capacitive loads. The high speed performance is achieved by means of a proprietary "Turbo-Driver" circuit that speeds up input stages by tapping the wider voltage swing at the output. Improved speed and drive capability are enhanced by matched rise and fall delay times. These matched delays maintain the integrity of input-to-output pulse-widths to reduce timing errors and clock skew problems. This improved performance is accompanied by a 10 fold reduction in supply currents over bipolar drivers, yet without the delay time problems commonly associated with CMOS devices. Dynamic switching losses are minimized with non-overlapped drive techniques.

Pinouts

EL7212
(8-PIN PDIP, SO)
TOP VIEW

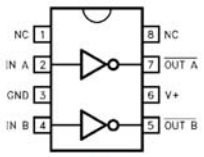

Inverting Drivers

EL7222
(8-PIN PDIP, SO)
TOP VIEW

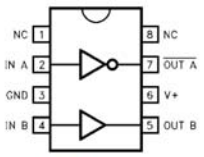

Complementary Drivers

EL7202
(8-PIN PDIP, SO)
TOP VIEW

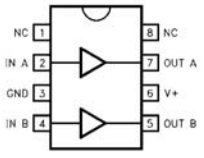

Non-Inverting Drivers

Manufactured under U.S. Patent Nos. 5,334,883, #5,341,047

Features

- Industry standard driver replacement
- Improved response times
- Matched rise and fall times
- Reduced clock skew
- Low output impedance
- Low input capacitance
- High noise immunity
- Improved clocking rate
- Low supply current
- Wide operating voltage range
- Pb-Free available (RoHS compliant)

Applications

- Clock/line drivers
- CCD Drivers
- Ultra-sound transducer drivers
- Power MOSFET drivers
- Switch mode power supplies
- Class D switching amplifiers
- Ultrasonic and RF generators
- Pulsed circuits

Ordering Information

PART NUMBER	PACKAGE	TAPE & REEL	PKG. DWG. #
EL7202CN	8-Pin PDIP	-	MDP0031
EL7202CS	8-Pin SO	-	MDP0027
EL7202CS-T7	8-Pin SO	7"	MDP0027
EL7202CS-T13	8-Pin SO	13"	MDP0027
EL7202CSZ (See Note)	8-Pin SO (Pb-free)		MDP0027
EL7202CSZ-T7 (See Note)	8-Pin SO (Pb-free)	7"	MDP0027
EL7202CSZ-T13 (See Note)	8-Pin SO (Pb-free)	13"	MDP0027
EL7212CN	8-Pin PDIP		MDP0031
EL7212CS	8-Pin SO		MDP0027
EL7212CS-T7	8-Pin SO	7"	MDP0027
EL7212CS-T13	8-Pin SO	13"	MDP0027
EL7212CSZ (See Note)	8-Pin SO (Pb-free)		MDP0027
EL7212CSZ-T7 (See Note)	8-Pin SO (Pb-free)	7"	MDP0027
EL7212CSZ-T13 (See Note)	8-Pin SO (Pb-free)	13"	MDP0027
EL7222CN	8-Pin PDIP		MDP0031
EL7222CS	8-Pin SO		MDP0027
EL7222CS-T7	8-Pin SO	7"	MDP0027
EL7222CS-T13	8-Pin SO	13"	MDP0027
EL7222CSZ (See Note)	8-Pin SO (Pb-free)		MDP0027
EL7222CSZ-T7 (See Note)	8-Pin SO (Pb-free)	7"	MDP0027
EL7222CSZ-T13 (See Note)	8-Pin SO (Pb-free)	13"	MDP0027

NOTE: Intersil Pb-free products employ special Pb-free material sets; molding compounds/die attach materials and 100% matte tin plate termination finish, which are RoHS compliant and compatible with both SnPb and Pb-free soldering operations. Intersil Pb-free products are MSL classified at Pb-free peak reflow temperatures that meet or exceed the Pb-free requirements of IPC/JEDEC J STD-020.

Absolute Maximum Ratings (T_A = 25°C)

Supply (V+ to Gnd) 16.5V
Input Pins . . . . . -0.3V to +0.3V above V+
Combined Peak Output Current 4A
Storage Temperature Range . . . . . .-65°C to +150°C
Ambient Operating Temperature . . . . . .-40°C to +85°C
Operating Junction Temperature . . . . . .125°C
Power Dissipation
SOIC 570mW
PDIP 1050mW

CAUTION: Stresses above those listed in "Absolute Maximum Ratings" may cause permanent damage to the device. This is a stress only rating and operation of the device at these or any other conditions above those indicated in the operational sections of this specification is not implied.

IMPORTANT NOTE: All parameters having Min/Max specifications are guaranteed. Typical values are for information purposes only. Unless otherwise noted, all tests are at the specified temperature and are pulsed tests, therefore: $T_J = T_C = T_A$

DC Electrical Specifications T_A = 25°C, V = 15V unless otherwise specified

PARAMETER	DESCRIPTION	TEST CONDITIONS	MIN	TYP	MAX	UNITS
INPUT						
V_{IH}	Logic "1" Input Voltage		2.4			V
I_{IH}	Logic "1" Input Current	@V+		0.1	10	µA
V_{IL}	Logic "0" Input Voltage				0.8	V
I_{IL}	Logic "0" Input Current	@0V		0.1	10	µA
V_{HVS}	Input Hysteresis			0.3		V
OUTPUT						
R_{OH}	Pull-Up Resistance	I_{OUT} = -100mA		3	6	Ω
R_{OL}	Pull-Down Resistance	I_{OUT} = +100mA		4	6	Ω
I_{PK}	Peak Output Current	Source Sink		2 2		A
I_{DC}	Continuous Output Current	Source/Sink	100			mA
POWER SUPPLY						
I_S	Power Supply Current	Inputs High/EL7202 Inputs High/EL7212 Inputs High/EL7222		4.5 1 2.5	7.5 2.5 5.0	mA
V_S	Operating Voltage		4.5		15	V

AC Electrical Specifications T_A = 25°C, V = 15V unless otherwise specified

PARAMETER	DESCRIPTION	TEST CONDITIONS	MIN	TYP	MAX	UNITS
SWITCHING CHARACTERISTICS						
t_R	Rise Time	C_L = 500pF C_L = 1000pF		7.5 10	 20	ns
t_F	Fall Time	C_L = 500pF C_L = 1000pF		10 13	 20	ns
t_{D1}	Turn-On Delay Time	See Timing Table		18	25	ns
t_{D2}	Turn-Off Delay Time	See Timing Table		20	25	ns

Timing Table

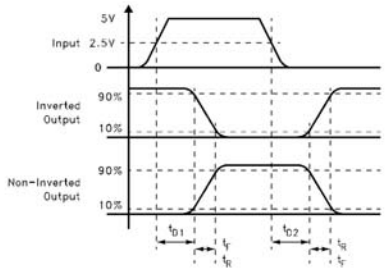

Standard Test Configuration

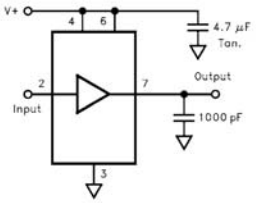

Simplified Schematic

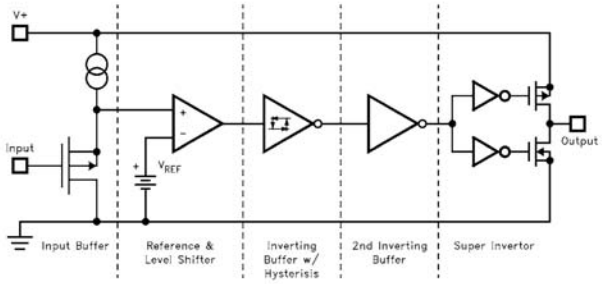

Typical Performance Curves

Max Power/Derating Curves

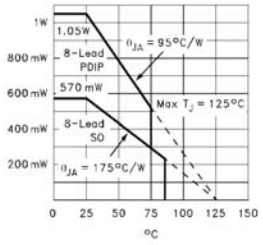

Switch Threshold vs Supply Voltage

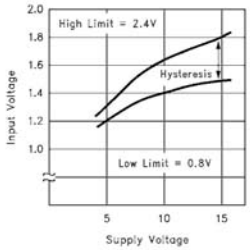

Input Current vs Voltage

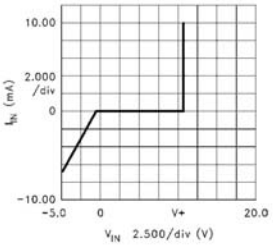

Peak Drive vs Supply Voltage

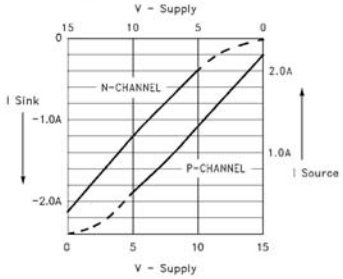

Quiescent Supply Current

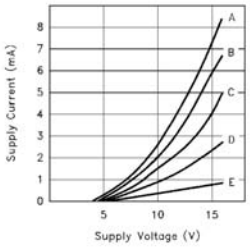

CASE:

Device	Input Level	Curve
EL7202	GND	A
EL7202	GND, V+	B
EL7202	V+	C
EL7212	GND	C
EL7212	GND, V+	D
EL7212	V+	E
EL7222	GND	B
EL7222	GND, V+	C
EL7222	V+	D

"ON" Resistance vs Supply Voltage

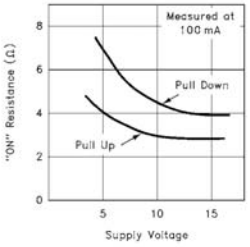

Typical Performance Curves (Continued)

Average Supply Current vs Voltage and Frequency

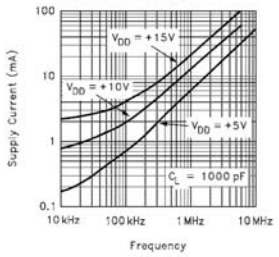

Average Supply Current vs Capacitive Load

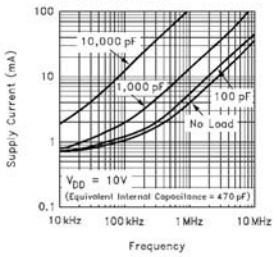

Rise/Fall Time vs Load

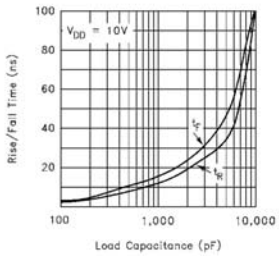

Rise/Fall Time vs Supply Voltage

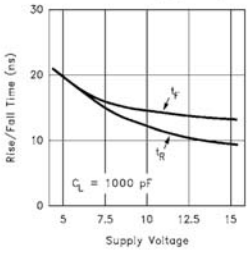

Propagation Delay vs Supply Voltage

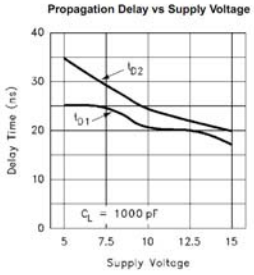

Rise/Fall Time vs Temperature

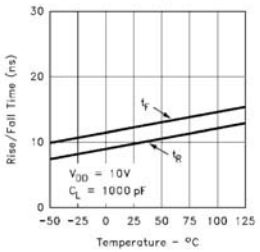

Delay vs Temperature

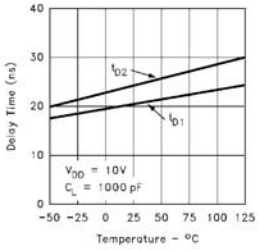

EL7212 Macro Model

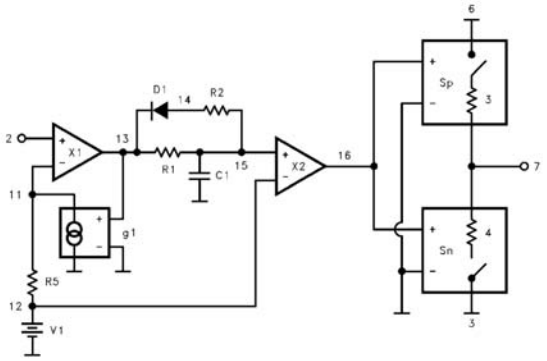


```
**** EL7212 model ****
*                    input
*                    |    gnd
*                    |    |    Vsupply
*                    |    |    |    Vout
.subckt M7212    2    3    6    7
V1 12 3 1.6
R1 13 15 1k
R2 14 15 5k
R5 11 12 100
C1 15 3 43.3 pF
D1 14 13 dmod
X1 13 11 2 3 comp1
X2 16 12 15 3 comp1
sp 6 7 16 3 spmod
sn 7 3 16 3 snmod
g1 11 0 13 0 938µ
.model dmod d
.model spmod vswitch ron3 roff2meg von1 voff1.5
.model snmod vswitch ron4 roff2meg von3 voff2
.ends M7212
.subckt comp1 out inp inm vss
e1 out vss table { (v(inp) v(inm))* 5000}   (0,0) (3.2,3.2)
Rout out vss 10meg
Rinp inp vss 10meg
Rinm inm vss 10meg
.ends comp1
```

Appendix F: Circuit Diagrams

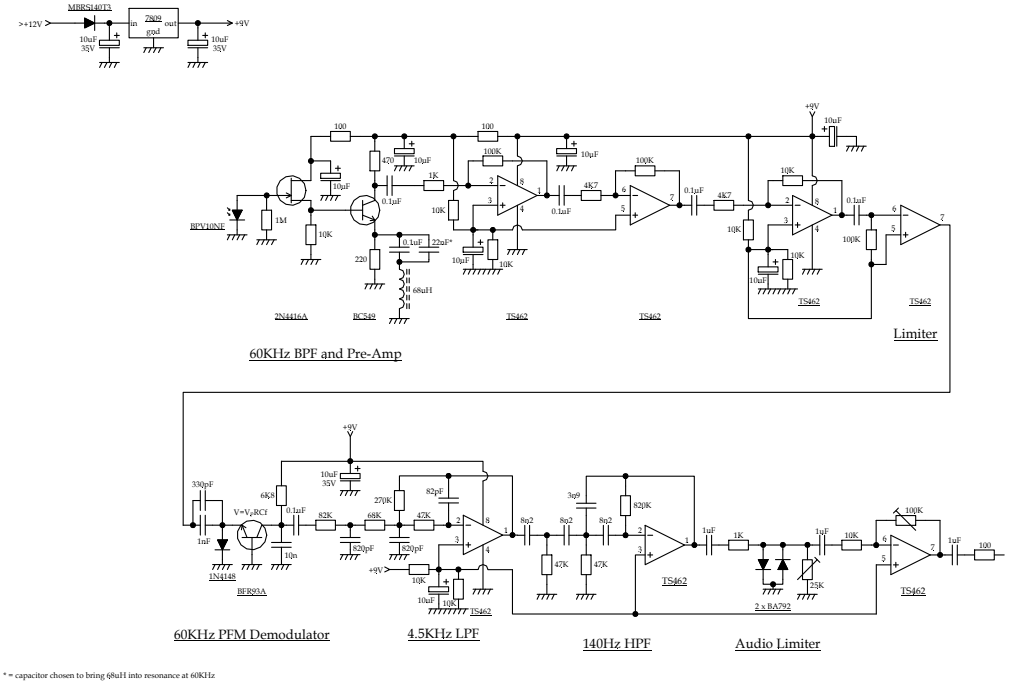

Figure F-1 60 kHz audio receiver

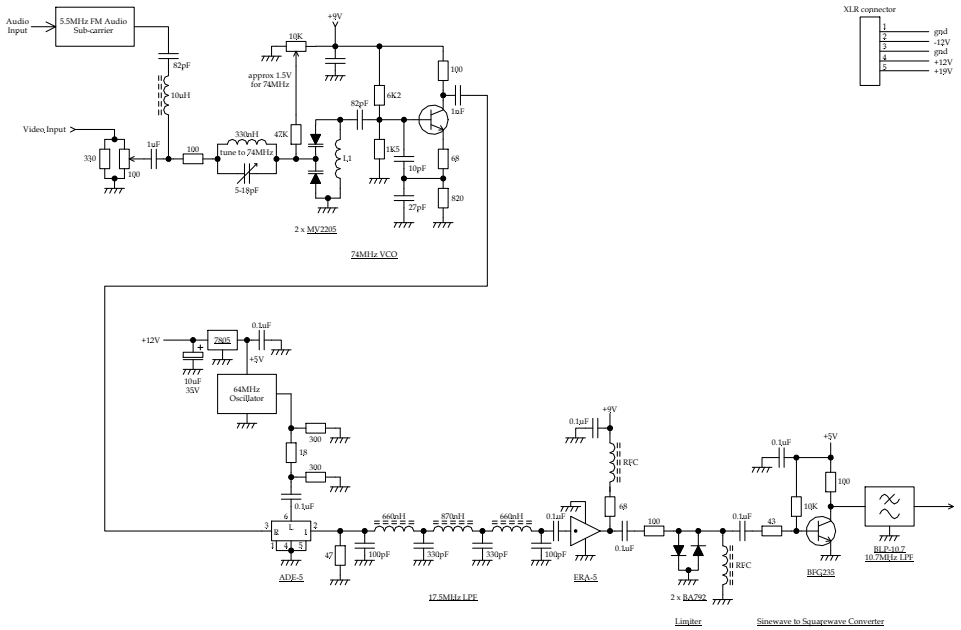

Figure F-2 Audio/video transmitter

Appendix G: Scintillometer Specifications

The following table shows the specifications of the Scintec BLS900 scintillometer [13].

	specifications	numerical
Transmitter	peak wavelength	880 nm (infrared)
	aperture diameter	150 mm each disk
	beam divergence	>10°
	pulse group repetition (PGR)	1 Hz, 5 Hz, 25 Hz or 125 Hz
	eye safe	yes
	operation voltage	12 VDC
	power consumption	110 W with PGR = 125 Hz 1 W with PGR = 1 Hz
	dimensions	135 mm x 180 mm x 364 mm
	weight	8.5 kg
Receiver	aperture diameter	140 mm
	field of view	8 mrad
	dimensions	160 mm x 160 mm x 590 mm
	weight	7.6 kg
Processing Unit (SPU)	storage capacity	up to 25 days (additional memory optional)
	internal clock	date and time
	dimensions	250 mm x 220 mm x 190 mm
	weight	4.7 kg
Receiver and SPU	operation voltage	12 VDC
	power consumption	9.6 W total
all	operation temperature	-25 to +50 °C

Appendix H: Kadina Meteorological Data for September 2011

The following table shows the meteorological data for September 2011. This is the closest Bureau of Meteorology recording station to Port Wakefield with recorded wind speeds.

Kadina, South Australia
September 2011 Daily Weather Observations

Date	Day	Temps		Rain	Evap	Sun	Max wind gust			9 am						3 pm					
		Min	Max				Dir	Spd	Time	Temp	RH	Cld	Dir	Spd	MSLP	Temp	RH	Cld	Dir	Spd	MSLP
		°C	°C	mm	mm	hours		km/h	local	°C	%	8th		km/h	hPa	°C	%	8th		km/h	hPa
1	Th	2.0	22.3	0			ENE	26	22:27	12.6	79		ENE	15	1024.1	22.2	36		NE	9	1020.9
2	Fr	5.1	23.9	0			NNE	46	13:54	15.4	59		NE	20	1020.9	23.7	30		N	30	1016.6
3	Sa	11.6	24.1	0			N	57	11:54	17.6	46		NNE	26	1013.0	21.5	35		NNE	24	1009.6
4	Su	5.1	17.8	0			WSW	39	02:05	15.1	78		WNW	4	1023.5	17.2	53		WSW	20	1022.1
5	Mo	0.1	20.9	0			WNW	30	22:23	13.1	81		NNE	7	1022.7	20.2	39		NNW	13	1017.4
6	Tu	6.2	15.7	0			SW	59	08:08	11.6	71		SW	22	1022.0	15.1	50		SW	22	1020.5
7	We	-0.9	18.3	0			N	35	11:37	11.6	80		NNE	19	1020.2	18.0	36		N	11	1016.7
8	Th	9.1	18.2	0			SE	37	04:51	12.3	75		ESE	19	1021.9	15.4	57		SSW	19	1020.7
9	Fr	3.7	17.6	0			SSW	57	15:16	13.1	78		S	31	1027.0	16.4	47		SSW	35	1026.4
10	Sa	5.6	15.5	0			WSW	46	15:41	13.1	67		SW	24	1028.8	14.2	61		SW	28	1025.4
11	Su	4.5	17.4	0			SW	41	16:43	12.9	86		SSW	17	1026.5	14.8	73		SW	24	1025.3
12	Mo	0.7	16.7	0.2			W	30	13:07	11.0	88		NNW	4	1029.6	14.3	73		SW	15	1027.4
13	Tu	-1.3	23.3	0.2			N	41	11:05	14.6	86		N	20	1026.0	22.7	31		N	17	1020.8
14	We	5.5	19.6	0			SSW	30	14:56	15.1	87		WSW	13	1024.8	18.7	54		S	20	1023.1
15	Th	2.9	27.4	0			N	24	11:41	15.6	71		ESE	11	1022.5	26.4	27		NE	11	1017.2
16	Fr	5.1	27.2	0			NW	24	11:40	17.7	76		ENE	11	1017.9	26.3	21		N	9	1014.1
17	Sa	6.3	30.8	0			SW	61	15:37	21.0	31		N	37	1009.3	24.2	41		WSW	35	1008.0
18	Su	5.3	23.8	0			NE	30	11:34	14.2	94		ENE	13	1018.0	22.5	28		NNE	20	1012.2
19	Mo	7.4	22.4	0			W	70	11:50	21.3	31		N	35	1000.6	18.8	54		WSW	35	1005.7
20	Tu	10.7	18.4	0			WSW	46	03:31	14.5	68		W	28	1016.9	17.9	49		SW	20	1017.6
21	We	2.6	23.8	0			NNE	31	11:51	16.1	80		N	11	1022.6	23.1	32		NNW	11	1017.7
22	Th	6.9	28.2	0			N	70	11:54	20.7	42		N	41	1013.0	26.6	30		WNW	28	1010.0
23	Fr	5.0	17.1	0			SSW	39	14:53	14.4	52		SSE	24	1024.1	15.2	49		SSW	28	1021.8
24	Sa	6.7	16.8	0			SW	39	13:38	13.7	56		SSW	17	1024.8	15.2	57		SSW	24	1023.2
25	Su	-1.1	18.5	0			W	31	15:48	12.0	69		E	17	1025.3	17.3	50		WSW	13	1020.1
26	Mo	3.0	25.1	0			N	41	11:55	17.4	36		NNE	15	1017.0	24.2	18		NNE	15	1010.5
27	Tu	8.6	30.8	0			N	48	09:58	24.3	24		NNE	17	1004.6	28.6	15		W	20	1001.3
28	We	8.7	21.6	3.6			W	83	23:23	13.2	97		E	13	1003.0	14.3	84		W	46	999.7
29	Th	9.1	17.5	5.8			WNW	78	03:30	13.8	84		SW	26	1008.0	16.4	54		SW	31	1009.7
30	Fr	9.9	16.0	3.0			WSW	61	14:32	12.1	90		WNW	30	1007.6	14.9	67		SW	35	1006.9
Statistics for September 2011																					
Mean		5.1	21.2							15.0	68			19	1018.9	19.5	45			22	1016.3
Lowest		-1.3	15.5	0						11.0	24		#	4	1000.6	14.2	15		#	9	999.7
Highest		11.6	30.8	5.8			W	83		24.3	97		N	41	1029.6	28.6	84		W	46	1027.4
Total				12.8																	

Appendix I: Link End Locations and GPS Co-ordinates

Table G-1 shows the GPS co-ordinates for the various positions of the interrogator and MRR for the trial dates Monday, 19 September through to Friday, 23 September. The range to the interrogator location at A2 is also listed.

Table G-1: GPS co-ordinates of boat and land positions during the trial

Position	Equip & Date	Range to A2	Bearing to A2	Latitude		Longitude	
A2	DMOI, All days	0 km		34 deg	16.62 S	138 deg	11.74 E
X4	MRR Mon & Tues	1.14 km	146 deg				
Boat position 1	MRR Wed	2.26 km	204 deg	34 deg	17.66 S	138 deg	10.97 E
Boat position 2	MRR Wed	3.07 km	204 deg	34 deg	18.04 S	138 deg	10.70 E
Boat position 3	MRR Wed	3.7 km	203 deg	34 deg	18.35 S	138 deg	10.52 E
Boat position 4	MRR Thu	3.8 km	184 deg	34 deg	18.63 S	138 deg	11.23 E
Boat postion 5	MRR Thu	3.2 km	187 deg	34 deg	18.29 S	138 deg	11.23 E
Boat postion 6	MRR Thu	2.36 km	214 deg	34 deg	17.57 S	138 deg	10.72 E
Boat postion 7	MRR Fri	2.2 km	216 deg	34 deg	17.48 S	138 deg	10.75 E
Boat postion 8	MRR Fri	1.92 km		34 deg	17.35 S	138 deg	10.86 E

Appendix J: Accelerometer Measurements

An inertial measurement device from Microstrain (model: Inertia-Link) was used to measure attitude, acceleration and angular rate in the roll, pitch and heading axes of the boat at anchor, sampled at selected boat positions. A summary of typical average angular rate of the boat's movement, along with the associated standard deviation is shown in Table H-1, for the pitch and roll directions.

Table H-1: Sampled average and standard deviations of the angular rate of boat movement in pitch and roll axes

Date	Distance (km)	Average Angular Speed (degrees/s)		Standard Deviation (degrees/s)	
		Pitch X	Roll Y	Pitch X	Roll Y
Wed 21/9/11	3.07	0.27	0.28	0.22	0.21
Wed 21/9/11	3.7	0.17	0.25	0.14	0.18
Thu 22/9/11	3.8	1.0	0.60	0.81	0.47
Fri 23/9/11	2.2	0.14	0.33	0.10	0.30

To enable the boat to remain stationary as much as possible during the measurements, two anchors situated at the bow and stern were used. However, due to shift in wind and tide directions during the measurements, it was not possible to entirely eliminate movement of the boat. Figure 24 shows a plot of representative measurements of the change in heading due to wind shift, experienced by the boat at anchor, at the various locations and days used for optical link demonstrations.

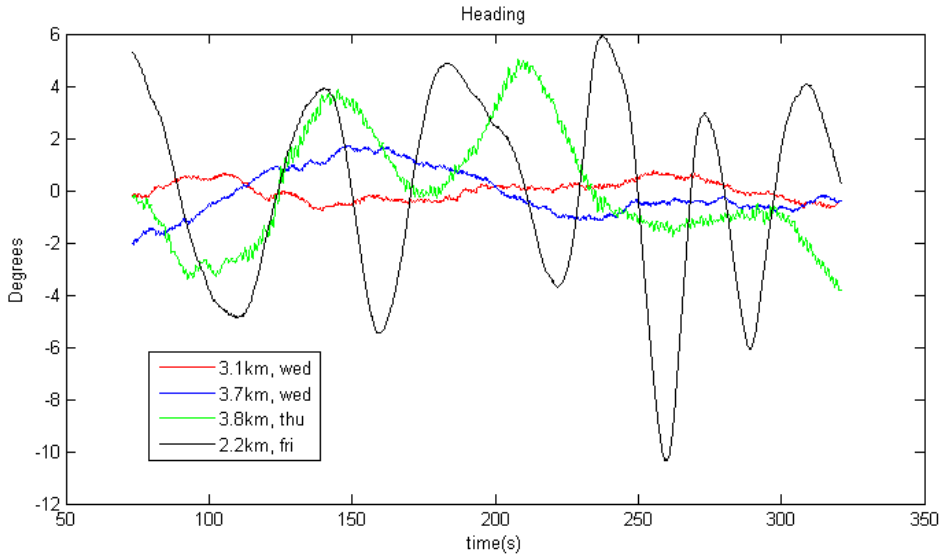

Figure 24: Representative heading data for the boat at anchor

DEFENCE SCIENCE AND TECHNOLOGY ORGANISATION
DOCUMENT CONTROL DATA

1. PRIVACY MARKING/CAVEAT (OF DOCUMENT)

2. TITLE

Maritime Laser Communications Trial 98152-19703

3. SECURITY CLASSIFICATION (FOR UNCLASSIFIED REPORTS THAT ARE LIMITED RELEASE USE (L) NEXT TO DOCUMENT CLASSIFICATION)

Document	(U)
Title	(U)
Abstract	(U)

4. AUTHOR(S)

Kenneth J. Grant, Kerry A. Mudge, Bradley A. Clare, Anna S. Perejma and Wayne M. Martinsen

5. CORPORATE AUTHOR

DSTO Defence Science and Technology Organisation
PO Box 1500
Edinburgh South Australia 5111 Australia

6a. DSTO NUMBER	6b. AR NUMBER	6c. TYPE OF REPORT	7. DOCUMENT DATE
DSTO-GD-0686	AR-015-320	General Document	June 2012

8. FILE NUMBER	9. TASK NUMBER	10. TASK SPONSOR	11. NO. OF PAGES	12. NO. OF REFERENCES
2012/1109668/1	07/009	NAV	48	16

13. DSTO Publications Repository

http://dspace.dsto.defence.gov.au/dspace/

14. RELEASE AUTHORITY

Chief, Command, Control, Communications and Intelligence Division

15. SECONDARY RELEASE STATEMENT OF THIS DOCUMENT

Approved for public release

OVERSEAS ENQUIRIES OUTSIDE STATED LIMITATIONS SHOULD BE REFERRED THROUGH DOCUMENT EXCHANGE, PO BOX 1500, EDINBURGH, SA 5111

16. DELIBERATE ANNOUNCEMENT

No Limitations

17. CITATION IN OTHER DOCUMENTS Yes

18. DSTO RESEARCH LIBRARY THESAURUS

Lasers, communications, laser communications, optical communications

19. ABSTRACT

This General Document describes the objectives, methodology, and results of Maritime Laser Communications Trial 98152-19703 held at Port Wakefield Proof & Experimental Establishment in September 2011. A novel analogue FM ship-to-shore communications system was used to demonstrate videπo and bidirectional audio transmission up to 3km.